Electronic Supplementary Material (ESI) for Dalton Transactions.
This journal is © The Royal Society of Chemistry 2021

Electronic Supporting Information

Syntheses and Structure of Dinuclear Metal Complexes Containing Naphthyl-Ir Bichromophore

Ryo Ohyama†, Masaki Mishima‡, Akiko Inagaki†*

†Department of Chemistry, Tokyo Metropolitan University, 1-1, Minami-Osawa, Hachioji, 192-0397 Tokyo, Japan.

‡Department of Molecular Biophysics, Tokyo University of Pharmacy and Life Sciences, School of Pharmacy, 1432-1 Horinouchi, Hachioji, Tokyo 192-0392, Japan.

Electronic Supporting Information

Experimental Details and Spectral Data

General Procedures.

Standard Schlenk and vacuum line techniques under a nitrogen atmosphere were employed for the reactions. Dichloromethane, acetone, THF, Et_2O, dimethoxyethane, hexane, ethylacetate, DMF, acetonitrile, MeOH, EtOH, and chloroform were treated with appropriate drying agents, distilled, and stored under N_2. 5,5'-dibromo-2,2'-bipyrimidine (bpm^{Br})[1] and [Pd(cod)MeCl][2] were prepared according to the published procedures. Other chemicals were purchased and used as received. ^1H (400 MHz), ^{31}P (162 MHz), ^{13}C (100 MHz) NMR spectra were acquired on a JEOL JNM-AL400 FT-NMR spectrometer and a Bruker AVANCE III 600 FT-NMR spectrometers. Electrospray ionization (ESI) mass spectra were recorded on a Bruker MicroTOF II mass spectrometers. UV−vis, and steady-state emission spectra were obtained on a JASCO V-670 and HITACHI F-7000 spectrometer, respectively. Gel Permeation Chromatography (GPC) spectra were recorded on SHIMADZU LC-10ADvp in THF vs. polystyrene standard. Emission lifetime was measured on Hamamatsu Photonics Quantaurus Tau.

Computational Details. DFT calculations were performed using the Gaussian-16 Revision A.03 quantum chemistry program package[i] at the B3LYP/LanL2DZ level[ii,iii.] We used the LanL2DZ pseudo-potential for Ir, 6-31G(d)[iv] split-valence basis set for N and the C bonded to Ir, 6-31G split-valence basis set for Br, and 3-21G[v] for the other C and H atoms. The orbital energies were determined by using minimized singlet geometries to approximate the ground state.

Preparation of 4-methyl-2-(3-(naphthalen-2-yl)phenyl)pyridine (L1).

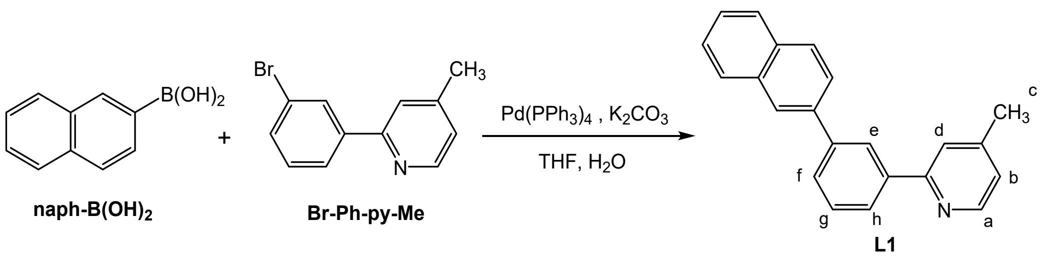

2-Naphthyl boronic acid (1.20 g, 0.00695 mol), K_2CO_3 (5.28 g, 0.0382 mol, 5.5 eq) and $Pd(PPh_3)_4$ (401.6 mg, 0.000348 mol, 0.05 eq) were dissolved in THF (110 mL) and H_2O (10 mL) in a 300 mL 2-necked flask. 2-(3-bromophenyl)-4-methylpyridine (1.7361 g, 0.00700 mol) was added and refluxed for 17 h at 100 °C under N_2. After cooled to room temperature, water (30 ml) was added and extracted with ethyl acetate (30 ml × 4) and then washed with brine. Collected organic layer was dried over $MgSO_4$. After removal of the solvent, crude product was purified by silica-gel column chromatography (CH_2Cl_2 / MeOH = 20 / 1) and HPLC to yield the target compound as a pale-yellow oil (0.533 g, 0.00180 mol, 26.0%). ^{1}H NMR (400 MHz, r.t., $CDCl_3$, δ / ppm): 8.59 (d, *J* = 4.8 Hz, 1 H, a), 8.34 (t, *J* = 1.8 Hz, 1 H, g), 8.14 (s, 1 H, d), 7.99 – 7.82 (m, 5 H, *naphthyl*), 7.77 (m, 1 H, f), 7.64 (s, 1 H, e), 7.58 (t, *J* = 8.0 Hz, 1 H, h), 7.53 – 7.46 (m, 2 H, *naphthyl*), 7.09 (dd, *J* = 4.8 Hz, 1 H, b) 2.44 (s, 3 H, c).

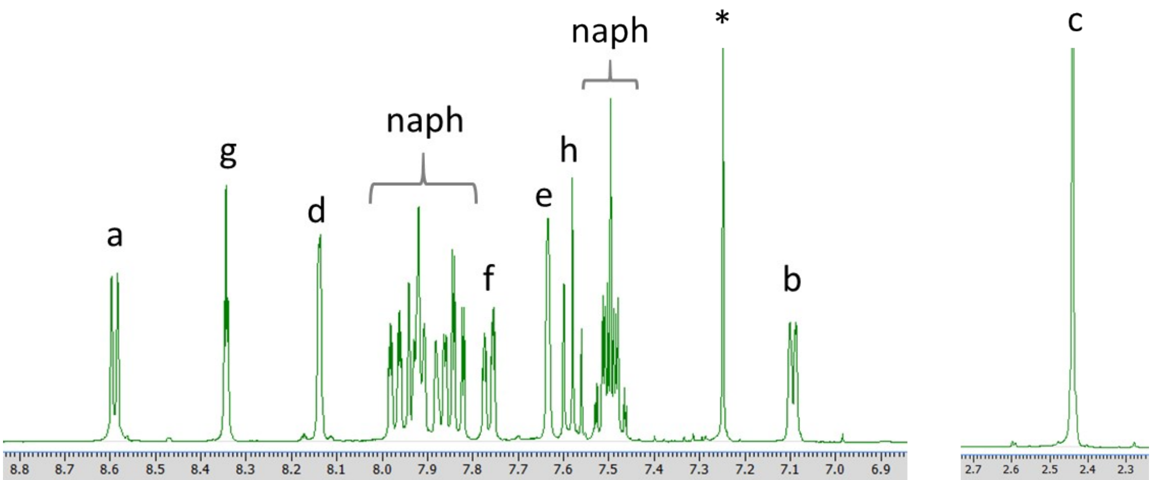

Figure S1. ^{1}H NMR spectra of **L1** (400 MHz, r.t., $CDCl_3$).

Preparation of 1-Me.

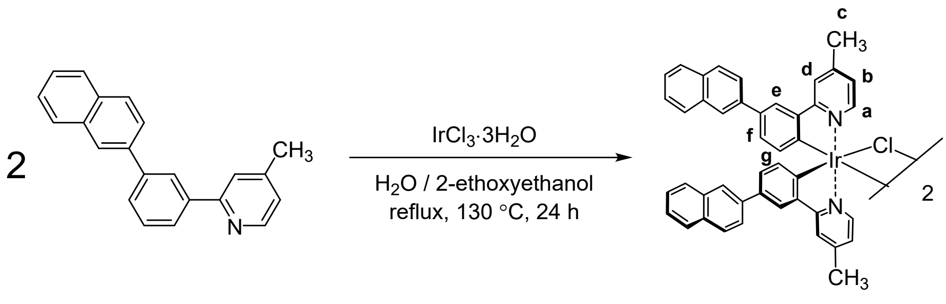

L1 **Ir-dimer**

[Ir(**L1**)$_2$(bpm^{Br})](BF_4) was prepared in a similar fashion to the published procedure for the synthesis of [Ir(C^N)$_2$(N^N)]$^+$.[3]

$IrCl_3$·3H_2O (0.317 g, 0.90 mmol) and 4-methyl-2-(3-(naphthalen-2-yl)phenyl)pyridine (**L1**: 0.533 g, 1.80 mmol) were dissolved in 2-ethoxyethanol (10 mL) and H_2O (3.3 mL), and refluxed under N_2 for 24 h at 130 ºC. The precipitate was filtered, washed with H_2O and EtOH, and then dried up to afford [Ir(**L1**)$_2$Cl]$_2$ as a yellow solid (0.511 g, 0.313 mmol, 69.5%). ^{1}H NMR (400 MHz, r.t., $CDCl_3$, δ / ppm) : 9.17 (d, *J* = 6.0 Hz, 4 H, a), 7.88 (s, 4 H, d), 7.83 – 7.77 (m, 16 H, *naphthyl*), 7.61 (dd, *J* = 8.4 Hz, 1.6 Hz, 4 H, f), 7.51 – 7.37 (m, 12 H, *naphthyl*), 6.97

(dd, J = 8.4 Hz, 1.6 Hz, 4 H, e), 6.67 (d, J = 6.0 Hz, 4 H, b), 6.17 (d, J = 8.0 Hz, 4 H, g), 2.71 (s, 12 H, c).

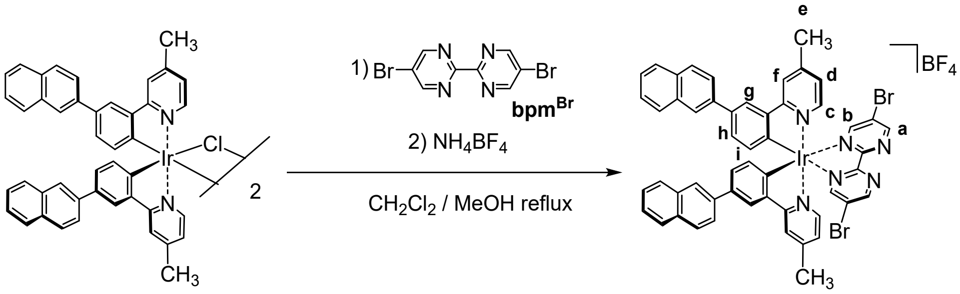

Ir-dimer **1-Me**

[Ir(**L1**)$_2$Cl]$_2$ (0.373 g, 0.229 mmol) and 5,5'-dibromo-2,2'-bipyrimidine (0.151 g, 0.480 mmol, 0.5eq) were dissolved in CH_2Cl_2 (18 mL) and MeOH (8 mL), and refluxed under N_2 for 5 h at. 50 ºC. The mixture was concentrated under vacuum and stirred with an excess amount of NH_4BF_4 (0.240 g, 2.29 mmol, 10 eq) at ambient temperature for 24 h. The precipitate was filtered and washed with EtOH, water, and Et_2O. The resulting solid was purified by column chromatography packed with neutral aluminum oxide (CH_2Cl_2 / CH_3CN = 2 : 1). The eluted pale orange band was collected and dried up under vacuum. The obtained solid was dissolved in CH_2Cl_2 and a slow diffusion of hexane yielded [Ir(**L1**)$_2$(bpm^{Br})](BF$_4$) as a dark-red solid (0.249 g, 0.211 mmol, 46.0%).

^{1}H NMR (400 MHz, CD_3CN, r.t., δ / ppm) : 9.27 (d, J = 2.8 Hz, 2 H, a), 8.26 (d, J = 2.8 Hz, 2 H, b), 8.23 (d, J = 1.6 Hz, 2 H, *naphthyl*) 8.17 (s, 4 H, g, *naphthyl*), 7.95 – 7.83 (m, 8 H, f, *naphthyl*), 7.68 (d, J = 6.0 Hz, 2 H, c), 7.52 – 7.45 (m, 4 H, *naphthyl*), 7.37 (dd, J = 8.0 Hz, 1.6 Hz, 2 H, h), 6.38 (d, J = 8.0 Hz, 2 H, i), 2.55 (s, 6 H, e). ESI-MS (CH_3CN) : m/z = 1069 [M – BF$_4$]$^+$. ^{13}C NMR (100 MHz, CD3CN, r.t., δ / ppm) ∶ δ 166.0 (C15), 160.6 (C14), 159.9 (C5), 158.3 (C12), 151.6 (C1), 149.8 (C3), 146.4 (C6), 145.2 (C8), 138.1 (C16), 135.9 (C19), 133.9 (C18), 132.5 (C11), 132.3 (C10), 129.1 (*naphthyl*), 128.5 (*naphthyl*), 128.0 (*naphthyl*), 127.6 (*naphthyl*), 126.5 (*naphthyl*), 126.0 (C9), 125.2 (C7), 124.9 (C17), 124.7 (s, C2), 123.5 (C4), 121.4 (C13), 20.4 (py-CH_3). Anal. Found (calcd for $C_{52}H_{36}BBr_2F_4IrN_6 + CH_2Cl_2$): C, 50.19 (50.18); H, 3.18 (3.02); N, 6.51 (6.62).

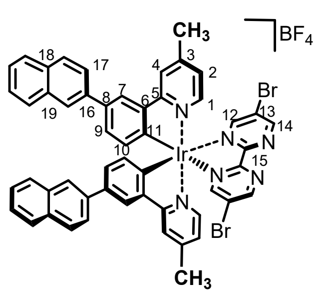

carbon label

Electronic Supporting Information

X-ray Structural Determinations.

The diffraction data of **1-Me** were collected on a Rigaku XtaLAB P100 diffractometer with graphite monochromated MoKα(λ=0.71073Å). The data were collected at a temperature of -175 ± 1°C to a maximum 2θ value of 55.1°. The crystal-to-detector distance was 45.00 mm. Readout was performed in the 0.172 mm pixel mode. Data were collected and processed using CrystalClear (Rigaku).[1] An empirical absorption correction was applied. The data were corrected for Lorentz and polarization effects.

The crystal structures were solved by direct method (SHELXS-97[2] or SHELXT[3]) and expanded using Fourier techniques, which are subsequently completed by Fourier recycling using the SHELXL 2014 program.[3] Non-hydrogen atoms were refined by anisotropic displacement parameters. Crystallographic data, data collection and refinement parameters for **1-Me** are listed in Table S1 and bond lengths and angles are listed in Table S2.

(1) CrystalClear: Data Collection and Processing Software, Rigaku Corporation (1998-2015). Tokyo 196-8666, Japan.

(2) SHELXS Version 2013/1: Sheldrick, G. M. (2008). Acta Cryst. A64, 112-122.

(3) SHELXT Version 2014/5: Sheldrick, G. M. (2014). Acta Cryst. A70, C1437.

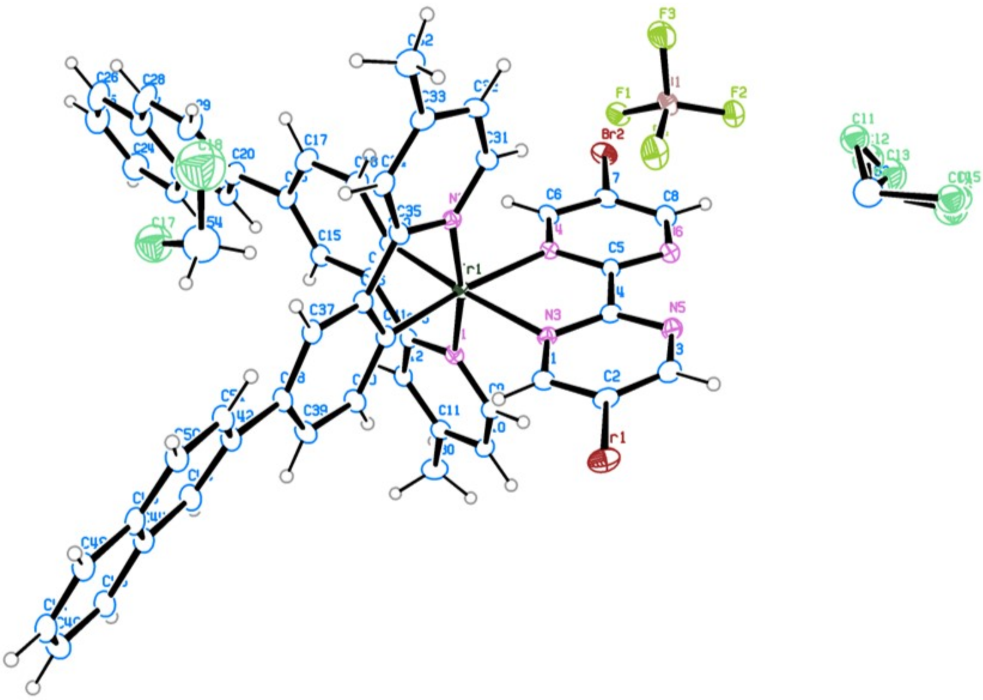

Figure S2. ORTEP diagram of **1-Me**.

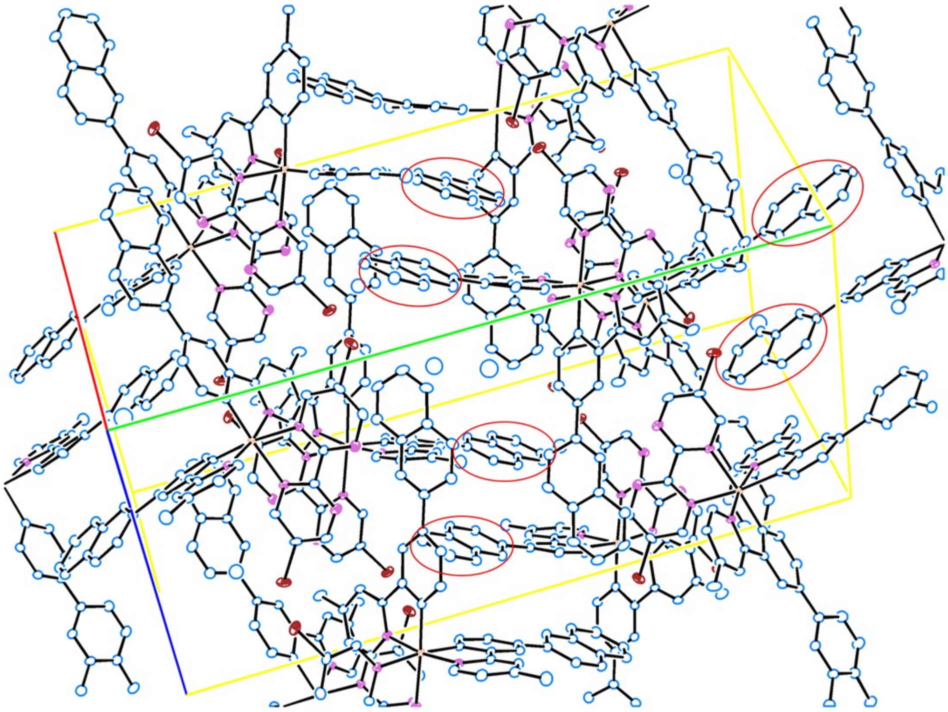

Figure S3.

ORTEP diagram (unit cell contents) of **1-Me** (BF_4 anions and a part of the solvent molecules are omitted for clarity)

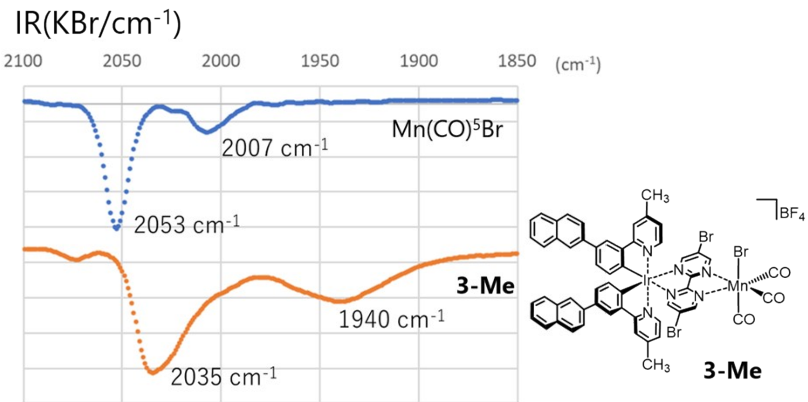

Figure S4. IR spectra of **3-Me** (KBr / cm^{-1}).

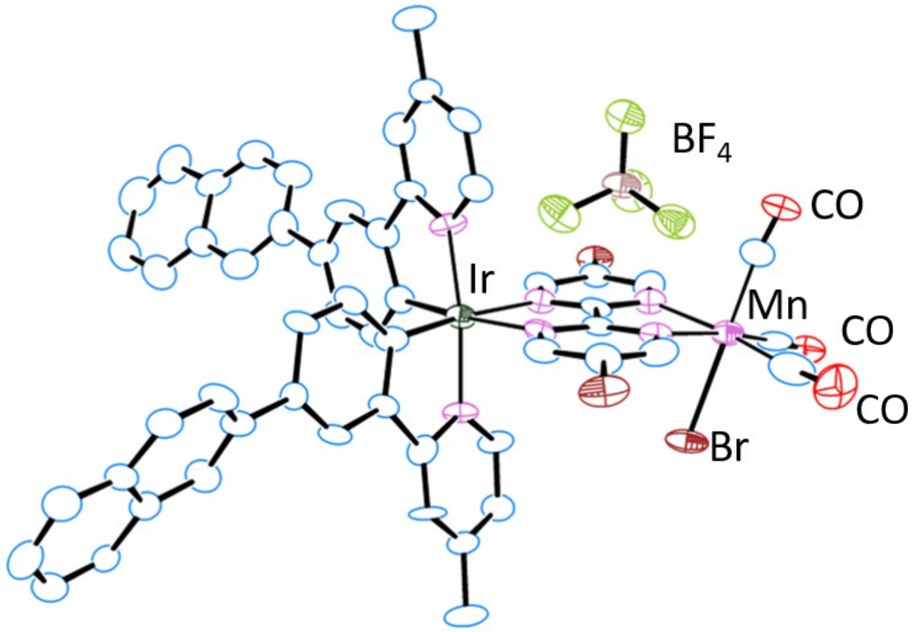

Figure S5. ORTEP diagram of **3-Me** (preliminary data, *R*1 = 0.15, I > 2σ).

Electronic Supporting Information

Table S1. Crystal data and structure refinement for **1-Me**.

Complex	**1-Me**	**3-Me**
Empirical formula	C54 H38 B Br2 Cl4 F4 Ir N6	C58 H36 B Br3 Cl4 F4 Ir Mn N6 O3
Formula weight	1351.53	1580.41
Temperature	98(2) K	98(2) K
Wavelength	0.71073 Å	0.71073 Å
Crystal system	Monoclinic	Triclinic
Space group	$P2_1$/n	P-1
Unit cell dimensions	a = 11.8536(3) Å b = 29.5795(7) Å c = 14.4519(3) Å	a = 10.8988(8) Å b = 13.9899(10) Å c = 20.7879(13) Å
	α= 90° β= 98.703(2)° γ = 90°	α= 73.462(6)° β= 83.849(6)° γ = 83.067(6)°
Volume	5008.8(2) Å^3	3007.4(4) Å^3
Z	4	2
Density (calculated)	1.792 Mg/m^3	1.745 Mg/m^3
Absorption coefficient	4.535 mm^{-1}	4.652 mm^{-1}
F(000)	2640	1532
Crystal size	0.730 x 0.280 x 0.080 mm^3	0.620 x 0.120 x 0.020 mm^3
Theta range for data collection	2.506 to 27.499°	2.537 to 27.500°
Index ranges	-14<=h<=15, -36<=k<=38, -17<=l<=18	-13<=h<=14, -17<=k<=17, -26<=l<=25
Reflections collected	41028	42430
Independent reflections	10680 [R(int) = 0.0337]	12565 [R(int) = 0.1797]
Completeness to theta = 27.50°	99.7 %	99.0 %
Refinement method	Full-matrix least-squares on F^2	Full-matrix least-squares on F^2
Data / restraints / parameters	10680 / 0 / 637	12565 / 0 / 709
Goodness-of-fit on F^2	1.110	1.220
Final R indices [I>2sigma(I)]	*R*1 = 0.0469, *wR*2 = 0.1268	*R*1 = 0.1468, *wR*2 = 0.3556
R indices (all data)	*R*1 = 0.0495, *wR*2 = 0.1279	*R*1 = 0.2208, *wR*2 = 0.3942
Largest diff. peak and hole	2.578 and -2.503 e.Å^{-3}	6.205 and -2.274 e.Å^{-3}

Electronic Supporting Information

Table S2. Bond lengths [Å] and angles [°] for **1-Me**.

Ir(1)-C(41)	2.002(6)	C(11)-C(30)	1.504(9)
Ir(1)-C(19)	2.003(6)	C(12)-C(13)	1.393(9)
Ir(1)-N(1)	2.052(5)	C(12)-H(12)	0.9500
Ir(1)-N(2)	2.054(5)	C(13)-C(14)	1.480(9)
Ir(1)-N(4)	2.156(5)	C(14)-C(15)	1.404(9)
Ir(1)-N(3)	2.166(5)	C(14)-C(19)	1.420(9)
N(1)-C(9)	1.341(8)	C(15)-C(16)	1.406(9)
N(1)-C(13)	1.366(7)	C(15)-H(15)	0.9500
N(2)-C(31)	1.343(8)	C(16)-C(17)	1.397(10)
N(2)-C(35)	1.366(8)	C(16)-C(20)	1.487(9)
N(3)-C(1)	1.347(8)	C(17)-C(18)	1.391(9)
N(3)-C(4)	1.351(8)	C(17)-H(17)	0.9500
N(4)-C(6)	1.338(8)	C(18)-C(19)	1.400(9)
N(4)-C(5)	1.352(8)	C(18)-H(18)	0.9500
N(5)-C(3)	1.328(9)	C(20)-C(21)	1.356(10)
N(5)-C(4)	1.335(8)	C(20)-C(29)	1.424(10)
N(6)-C(5)	1.328(8)	C(21)-C(22)	1.418(9)
N(6)-C(8)	1.349(9)	C(21)-H(21)	0.9500
C(1)-C(2)	1.396(9)	C(22)-C(27)	1.408(10)
C(1)-H(1)	0.9500	C(22)-C(23)	1.450(10)
C(2)-C(3)	1.372(10)	C(23)-C(24)	1.342(10)
C(2)-Br(1)	1.866(6)	C(23)-H(23)	0.9500
C(3)-H(3)	0.9500	C(24)-C(25)	1.402(12)
C(4)-C(5)	1.485(8)	C(24)-H(24)	0.9500
C(6)-C(7)	1.382(9)	C(25)-C(26)	1.338(12)
C(6)-H(6)	0.9500	C(25)-H(25)	0.9500
C(7)-C(8)	1.366(10)	C(26)-C(27)	1.436(10)
C(7)-Br(2)	1.875(6)	C(26)-H(26)	0.9500
C(8)-H(8)	0.9500	C(27)-C(28)	1.417(12)
C(9)-C(10)	1.376(9)	C(28)-C(29)	1.374(11)
C(9)-H(9)	0.9500	C(28)-H(28)	0.9500
C(10)-C(11)	1.389(8)	C(29)-H(29)	0.9500
C(10)-H(10)	0.9500	C(30)-H(30)	0.9800
C(11)-C(12)	1.381(9)	C(30)-H(30A)	0.9800

C(30)-H(30B)	0.9800	C(50)-H(50)	0.9500
C(31)-C(32)	1.376(9)	C(51)-H(51)	0.9500
C(31)-H(31)	0.9500	C(52)-H(52)	0.9800
C(32)-C(33)	1.393(10)	C(52)-H(52A)	0.9800
C(32)-H(32)	0.9500	C(52)-H(52B)	0.9800
C(33)-C(34)	1.395(10)	B(1)-F(3)	1.374(9)
C(33)-C(52)	1.504(9)	B(1)-F(2)	1.379(9)
C(34)-C(35)	1.382(9)	B(1)-F(4)	1.401(9)
C(34)-H(34)	0.9500	B(1)-F(1)	1.403(8)
C(35)-C(36)	1.477(8)	C(53)-Cl(6)	1.650(17)
C(36)-C(37)	1.398(9)	C(53)-Cl(2)	1.758(14)
C(36)-C(41)	1.405(8)	C(53)-Cl(1)	1.772(13)
C(37)-C(38)	1.404(9)	C(53)-Cl(4)	1.781(14)
C(37)-H(37)	0.9500	C(53)-Cl(5)	1.816(14)
C(38)-C(39)	1.400(9)	C(53)-Cl(3)	1.892(15)
C(38)-C(42)	1.499(9)	Cl(1)-Cl(2)	0.540(13)
C(39)-C(40)	1.384(9)	Cl(1)-Cl(3)	1.082(15)
C(39)-H(39)	0.9500	Cl(2)-Cl(3)	0.555(14)
C(40)-C(41)	1.409(9)	Cl(4)-Cl(6)	0.526(15)
C(40)-H(40)	0.9500	Cl(7)-C(54)	1.647(14)
C(42)-C(43)	1.393(9)	Cl(8)-C(54)	1.757(14)
C(42)-C(51)	1.413(9)	C(54)-H(54)	0.9900
C(43)-C(44)	1.420(9)	C(54)-H(54A)	0.9900
C(43)-H(43)	0.9500		
C(44)-C(49)	1.421(9)	C(41)-Ir(1)-C(19)	88.7(2)
C(44)-C(45)	1.432(9)	C(41)-Ir(1)-N(1)	94.5(2)
C(45)-C(46)	1.350(10)	C(19)-Ir(1)-N(1)	80.1(2)
C(45)-H(45)	0.9500	C(41)-Ir(1)-N(2)	79.9(2)
C(46)-C(47)	1.412(11)	C(19)-Ir(1)-N(2)	92.2(2)
C(46)-H(46)	0.9500	N(1)-Ir(1)-N(2)	170.6(2)
C(47)-C(48)	1.356(10)	C(41)-Ir(1)-N(4)	171.9(2)
C(47)-H(47)	0.9500	C(19)-Ir(1)-N(4)	99.4(2)
C(48)-C(49)	1.425(9)	N(1)-Ir(1)-N(4)	86.80(19)
C(48)-H(48)	0.9500	N(2)-Ir(1)-N(4)	99.82(19)
C(49)-C(50)	1.413(10)	C(41)-Ir(1)-N(3)	96.1(2)
C(50)-C(51)	1.364(9)	C(19)-Ir(1)-N(3)	175.1(2)

Electronic Supporting Information

N(1)-Ir(1)-N(3)	100.50(19)	C(8)-C(7)-Br(2)	120.8(5)
N(2)-Ir(1)-N(3)	87.62(19)	C(6)-C(7)-Br(2)	120.1(5)
N(4)-Ir(1)-N(3)	75.83(19)	N(6)-C(8)-C(7)	121.8(6)
C(9)-N(1)-C(13)	119.0(5)	N(6)-C(8)-H(8)	119.1
C(9)-N(1)-Ir(1)	124.5(4)	C(7)-C(8)-H(8)	119.1
C(13)-N(1)-Ir(1)	116.5(4)	N(1)-C(9)-C(10)	122.1(6)
C(31)-N(2)-C(35)	119.1(5)	N(1)-C(9)-H(9)	118.9
C(31)-N(2)-Ir(1)	124.3(4)	C(10)-C(9)-H(9)	118.9
C(35)-N(2)-Ir(1)	116.3(4)	C(9)-C(10)-C(11)	120.1(6)
C(1)-N(3)-C(4)	117.6(5)	C(9)-C(10)-H(10)	120.0
C(1)-N(3)-Ir(1)	125.8(4)	C(11)-C(10)-H(10)	120.0
C(4)-N(3)-Ir(1)	116.0(4)	C(12)-C(11)-C(10)	117.8(6)
C(6)-N(4)-C(5)	117.5(5)	C(12)-C(11)-C(30)	121.5(6)
C(6)-N(4)-Ir(1)	125.8(4)	C(10)-C(11)-C(30)	120.6(6)
C(5)-N(4)-Ir(1)	116.4(4)	C(11)-C(12)-C(13)	120.5(6)
C(3)-N(5)-C(4)	116.2(6)	C(11)-C(12)-H(12)	119.8
C(5)-N(6)-C(8)	116.0(6)	C(13)-C(12)-H(12)	119.8
N(3)-C(1)-C(2)	119.5(6)	N(1)-C(13)-C(12)	120.5(6)
N(3)-C(1)-H(1)	120.2	N(1)-C(13)-C(14)	113.6(5)
C(2)-C(1)-H(1)	120.2	C(12)-C(13)-C(14)	125.9(5)
C(3)-C(2)-C(1)	118.3(6)	C(15)-C(14)-C(19)	122.2(6)
C(3)-C(2)-Br(1)	121.0(5)	C(15)-C(14)-C(13)	123.6(6)
C(1)-C(2)-Br(1)	120.7(5)	C(19)-C(14)-C(13)	114.1(5)
N(5)-C(3)-C(2)	122.8(6)	C(14)-C(15)-C(16)	120.1(6)
N(5)-C(3)-H(3)	118.6	C(14)-C(15)-H(15)	119.9
C(2)-C(3)-H(3)	118.6	C(16)-C(15)-H(15)	119.9
N(5)-C(4)-N(3)	125.6(6)	C(17)-C(16)-C(15)	117.7(6)
N(5)-C(4)-C(5)	118.9(6)	C(17)-C(16)-C(20)	120.9(6)
N(3)-C(4)-C(5)	115.5(5)	C(15)-C(16)-C(20)	121.4(6)
N(6)-C(5)-N(4)	125.7(6)	C(18)-C(17)-C(16)	121.9(6)
N(6)-C(5)-C(4)	118.6(5)	C(18)-C(17)-H(17)	119.0
N(4)-C(5)-C(4)	115.6(5)	C(16)-C(17)-H(17)	119.0
N(4)-C(6)-C(7)	119.9(6)	C(17)-C(18)-C(19)	121.7(6)
N(4)-C(6)-H(6)	120.0	C(17)-C(18)-H(18)	119.1
C(7)-C(6)-H(6)	120.0	C(19)-C(18)-H(18)	119.1
C(8)-C(7)-C(6)	119.0(6)	C(18)-C(19)-C(14)	116.2(6)

C(18)-C(19)-Ir(1)	128.2(5)	H(30)-C(30)-H(30B)	109.5
C(14)-C(19)-Ir(1)	115.6(4)	H(30A)-C(30)-H(30B)	109.5
C(21)-C(20)-C(29)	118.2(6)	N(2)-C(31)-C(32)	122.4(6)
C(21)-C(20)-C(16)	122.7(6)	N(2)-C(31)-H(31)	118.8
C(29)-C(20)-C(16)	119.1(6)	C(32)-C(31)-H(31)	118.8
C(20)-C(21)-C(22)	121.9(6)	C(31)-C(32)-C(33)	119.8(6)
C(20)-C(21)-H(21)	119.1	C(31)-C(32)-H(32)	120.1
C(22)-C(21)-H(21)	119.1	C(33)-C(32)-H(32)	120.1
C(27)-C(22)-C(21)	119.6(6)	C(32)-C(33)-C(34)	117.4(6)
C(27)-C(22)-C(23)	118.1(6)	C(32)-C(33)-C(52)	121.1(6)
C(21)-C(22)-C(23)	122.2(6)	C(34)-C(33)-C(52)	121.4(7)
C(24)-C(23)-C(22)	120.6(7)	C(35)-C(34)-C(33)	120.8(6)
C(24)-C(23)-H(23)	119.7	C(35)-C(34)-H(34)	119.6
C(22)-C(23)-H(23)	119.7	C(33)-C(34)-H(34)	119.6
C(23)-C(24)-C(25)	121.0(7)	N(2)-C(35)-C(34)	120.4(6)
C(23)-C(24)-H(24)	119.5	N(2)-C(35)-C(36)	113.1(5)
C(25)-C(24)-H(24)	119.5	C(34)-C(35)-C(36)	126.4(6)
C(26)-C(25)-C(24)	120.6(7)	C(37)-C(36)-C(41)	122.0(6)
C(26)-C(25)-H(25)	119.7	C(37)-C(36)-C(35)	123.2(6)
C(24)-C(25)-H(25)	119.7	C(41)-C(36)-C(35)	114.8(5)
C(25)-C(26)-C(27)	121.3(8)	C(36)-C(37)-C(38)	120.4(6)
C(25)-C(26)-H(26)	119.3	C(36)-C(37)-H(37)	119.8
C(27)-C(26)-H(26)	119.3	C(38)-C(37)-H(37)	119.8
C(22)-C(27)-C(28)	118.5(7)	C(39)-C(38)-C(37)	117.8(6)
C(22)-C(27)-C(26)	118.4(7)	C(39)-C(38)-C(42)	120.6(6)
C(28)-C(27)-C(26)	123.1(8)	C(37)-C(38)-C(42)	121.5(6)
C(29)-C(28)-C(27)	120.1(7)	C(40)-C(39)-C(38)	121.6(6)
C(29)-C(28)-H(28)	119.9	C(40)-C(39)-H(39)	119.2
C(27)-C(28)-H(28)	119.9	C(38)-C(39)-H(39)	119.2
C(28)-C(29)-C(20)	121.6(7)	C(39)-C(40)-C(41)	121.5(6)
C(28)-C(29)-H(29)	119.2	C(39)-C(40)-H(40)	119.3
C(20)-C(29)-H(29)	119.2	C(41)-C(40)-H(40)	119.3
C(11)-C(30)-H(30)	109.5	C(36)-C(41)-C(40)	116.8(6)
C(11)-C(30)-H(30A)	109.5	C(36)-C(41)-Ir(1)	115.7(4)
H(30)-C(30)-H(30A)	109.5	C(40)-C(41)-Ir(1)	127.5(5)
C(11)-C(30)-H(30B)	109.5	C(43)-C(42)-C(51)	117.8(6)

C(43)-C(42)-C(38)	121.0(6)
C(51)-C(42)-C(38)	121.1(6)
C(42)-C(43)-C(44)	121.3(6)
C(42)-C(43)-H(43)	119.4
C(44)-C(43)-H(43)	119.4
C(43)-C(44)-C(49)	119.6(6)
C(43)-C(44)-C(45)	122.3(6)
C(49)-C(44)-C(45)	118.1(6)
C(46)-C(45)-C(44)	121.4(7)
C(46)-C(45)-H(45)	119.3
C(44)-C(45)-H(45)	119.3
C(45)-C(46)-C(47)	120.6(7)
C(45)-C(46)-H(46)	119.7
C(47)-C(46)-H(46)	119.7
C(48)-C(47)-C(46)	119.8(6)
C(48)-C(47)-H(47)	120.1
C(46)-C(47)-H(47)	120.1
C(47)-C(48)-C(49)	121.7(7)
C(47)-C(48)-H(48)	119.1
C(49)-C(48)-H(48)	119.1
C(50)-C(49)-C(44)	118.0(6)
C(50)-C(49)-C(48)	123.6(6)
C(44)-C(49)-C(48)	118.4(6)
C(51)-C(50)-C(49)	121.3(6)
C(51)-C(50)-H(50)	119.4
C(49)-C(50)-H(50)	119.4
C(50)-C(51)-C(42)	122.0(6)
C(50)-C(51)-H(51)	119.0
C(42)-C(51)-H(51)	119.0
C(33)-C(52)-H(52)	109.5
C(33)-C(52)-H(52A)	109.5
H(52)-C(52)-H(52A)	109.5
C(33)-C(52)-H(52B)	109.5
H(52)-C(52)-H(52B)	109.5
H(52A)-C(52)-H(52B)	109.5
F(3)-B(1)-F(2)	110.2(6)
F(3)-B(1)-F(4)	110.7(6)
F(2)-B(1)-F(4)	109.7(6)
F(3)-B(1)-F(1)	108.7(6)
F(2)-B(1)-F(1)	109.8(6)
F(4)-B(1)-F(1)	107.7(5)
Cl(6)-C(53)-Cl(2)	105.7(9)
Cl(6)-C(53)-Cl(1)	115.4(8)
Cl(2)-C(53)-Cl(1)	17.6(4)
Cl(6)-C(53)-Cl(4)	17.1(6)
Cl(2)-C(53)-Cl(4)	118.0(7)
Cl(1)-C(53)-Cl(4)	123.6(7)
Cl(6)-C(53)-Cl(5)	8.3(7)
Cl(2)-C(53)-Cl(5)	107.1(8)
Cl(1)-C(53)-Cl(5)	114.4(7)
Cl(4)-C(53)-Cl(5)	11.6(5)
Cl(6)-C(53)-Cl(3)	91.8(8)
Cl(2)-C(53)-Cl(3)	17.0(5)
Cl(1)-C(53)-Cl(3)	34.1(5)
Cl(4)-C(53)-Cl(3)	106.3(7)
Cl(5)-C(53)-Cl(3)	94.7(7)
Cl(2)-Cl(1)-Cl(3)	9.1(17)
Cl(2)-Cl(1)-C(53)	79.7(16)
Cl(3)-Cl(1)-C(53)	79.0(8)
Cl(1)-Cl(2)-Cl(3)	162(3)
Cl(1)-Cl(2)-C(53)	82.7(17)
Cl(3)-Cl(2)-C(53)	95(2)
Cl(2)-Cl(3)-Cl(1)	8.9(16)
Cl(2)-Cl(3)-C(53)	67.6(18)
Cl(1)-Cl(3)-C(53)	66.8(7)
Cl(6)-Cl(4)-C(53)	67(2)
Cl(4)-Cl(6)-C(53)	96(2)
Cl(7)-C(54)-Cl(8)	117.5(9)
Cl(7)-C(54)-H(54)	107.9
Cl(8)-C(54)-H(54)	107.9
Cl(7)-C(54)-H(54A)	107.9
Cl(8)-C(54)-H(54A)	107.9

H(54)-C(54)-H(54A)	107.2

Symmetry transformations used to generate equivalent atoms:

Palladation of [Ir(**L1**)$_2$(bpm^{Br})](BF$_4$) was implemented in a similar fashion to the published procedure for the synthesis of the Ru-Pd complex.[4] [Ir(**L1**)$_2$(bpm^{Br})](BF$_4$) (57.2 mg, 0.0483 mmol) and [PdMeCl(cod)] (15.4 mg, 0.0580 mmol, 1.2 eq) were dissolved in CH_2Cl_2 (3 mL) and stirred at ambient temperature for 3 h. The solvent was removed under reduced pressure and the resulting solid was precipitated with CH_2Cl_2-Et_2O and washed with toluene and Et_2O, which yielded [Ir(Ph^{naph}py^{Me})$_2$(bpm^{Br})PdMeCl](BF$_4$)$_2$ as a brownish-red solid (43.9 mg, 0.0327 mmol, 67.7%).

^{1}H NMR (400 MHz, r.t., CD_3NO_2, δ / ppm) : δ 9.33, 9.18 (s, 2 H, H14), 8.82, 8.78 (s, 2 H, H12), 8.28 (s, 2 H, H7), 8.17 (d, J = 12.8 Hz, 2 H, *naphthyl*), 7.97 – 7.79 (m, 10 H, *naphthyl,* H1, H4), 7.54 – 7.47 (m, 4 H, *naphthyl*), 7.41 (d, J = 7.2 Hz, 2 H, H9), 7.05 (d, J = 5.6 Hz, 2 H, H2), 6.50 (dd, J = 7.2 Hz, 3.6 Hz, 2 H, H10), 2.61 (s, 6 H, H3), 1.17 (s, 3 H, Pd-CH_3).

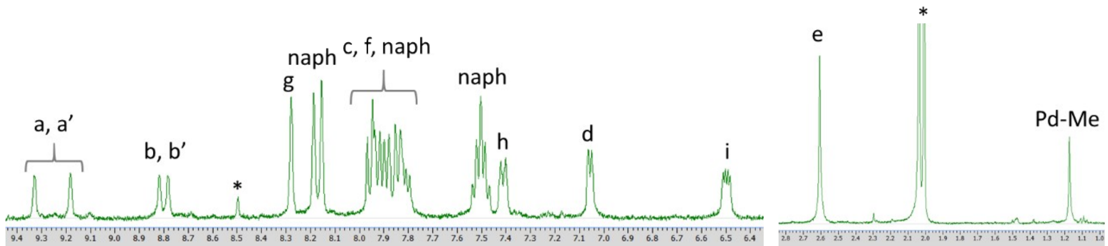

Figure S6. ^{1}H NMR spectra of [Ir(**L1**)$_2$(bpm^{Br})PdMeCl](BF$_4$)$_2$ (400 MHz, r.t., CD_3NO_2).

Preparation of [Ir(**L1**)$_2$(bpm^{Br})PdMe(Me$_2$CO)](BF$_4$)$_2$ (**2-Me**).

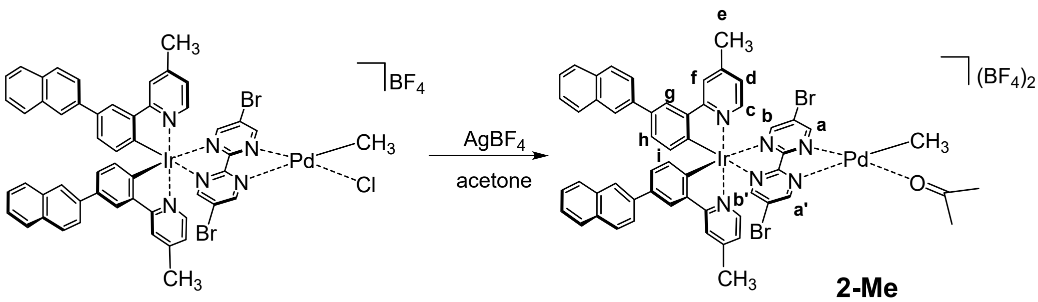

[Ir(**L1**)$_2$(bpm^{Br})PdMeCl](BF$_4$)$_2$ (43.9 mg, 0.0327 mmol) was dissolved in acetone (5 mL) and acetone (1 mL) solution of $AgBF_4$ (6.69 mg, 0.0344 mmol, 1.05 eq) was added. The mixture was stirred at ambient temperature for 1 h. The resulting solution was filtered through Celite and the filtrate was concentrated under vacuum. Then the resulting solution was precipitated with CH_2Cl_2-Et_2O. It gave the target compound **1** as a brownish-red solid (37.0 mg, 0.0255 mmol, 78.1%).

^{1}H NMR (400 MHz, CD_3NO_2, r.t., δ / ppm) : 9.16 (brs, 2 H, a, a'), 8.86 (brs, 2 H, b, b'), 8.28 (s, 2 H, g), 8.20 – 8.15 (m, 4 H, *naphthyl*), 7.97 –7.81 (m, 10 H, c, f, *naphthyl*), 7.54 – 7.47 (m, 4 H, *naphthyl*), 7.42 (d, J = 8.0 Hz, 2 H, h), 7.08 (d, J = 5.6 Hz, 2 H, d), 6.48 (d, J = 8.0 Hz, 2 H, i), 2.62 (s, 6 H, e), 1.48 (brs, 3 H, Pd-CH_3).

^{13}C NMR (100 MHz, CD_3CN, r.t., δ / ppm) : δ 166.0 (C15), 160.6 (C14), 159.9 (C5), 158.2 (C12), 151.6 (C1), 149.8 (C3), 146.3 (C6), 145.2 (C8), 138.1 (C16), 135.9 (C19), 133.9 (C18), 132.5 (C11), 132.3 (C10), 129.1 (*naphthyl*), 128.5 (*naphthyl*), 128.0 (*naphthyl*), 127.6 (*naphthyl*), 126.5 (*naphthyl*), 126.0 (C9), 125.2 (C7), 124.9 (C17), 124.7 (C2), 123.5 (C4), 121.4 (C13), 20.4 (py-CH_3), 14.6 (Pd-Me).

Anal. Found (calcd for $C_{56}H_{45}B_2Br_2F_8IrN_6OPd$): C, 46.70 (46.39); H, 3.39 (3.13); N, 5.57 (5.80).

The proton and carbon signals of a coordinating solvent were each overlapped with the residual proton signals and the carbon signals of CD_3CN, respectively.

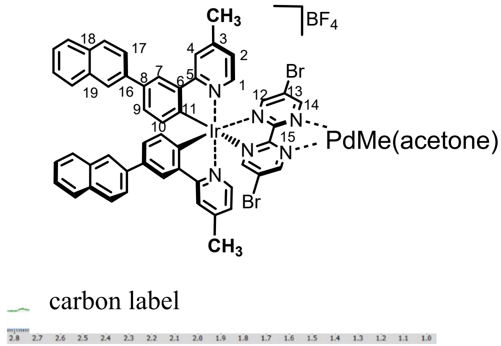

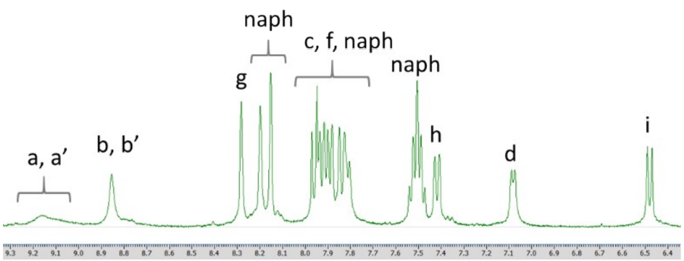

Figure S7. ^{1}H NMR spectra of **2-Me** (400 MHz, r.t., CD_3NO_2).

Preparation of [Ir(**L1**)$_2$(bpm^{Br})Mn(CO)$_3$Br](BF_4) (**3-Me**).

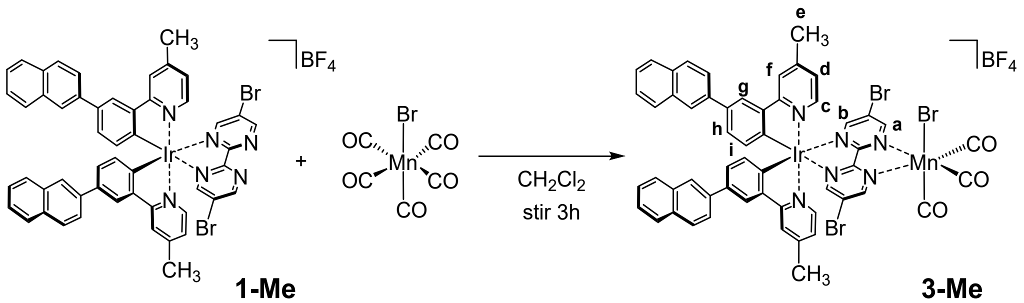

[Ir(**L1**)$_2$(bpm^{Br})](BF_4) (1.05 eq, 28.0 mg, 0.0236 mmol) and Mn(CO)$_5$Br (1.0 eq, 6.20 mg, 0.0225 mmol) were dissolved in CH_2Cl_2 (3 mL) and stirred at ambient temperature for 3 h. The solvent was removed under reduced pressure and the resulting solid was precipitated with CH_2Cl_2-hexane, which yielded [Ir(**L1**)$_2$(bpm^{Br}) Mn(CO)$_3$Br](BF_4) as a brownish-red solid (22.0 mg, 0.0157 mmol, 69.4%)

^{1}H NMR (400 MHz, CD_3CN, r.t., δ / ppm) : 8.23-8.17

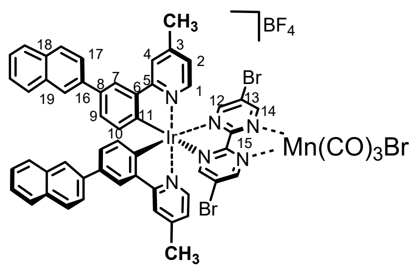

carbon label

(m, 8 H, a, g, *naphthyl*), 7.94 (m, 10 H, b, f, *naphthyl*), 7.67 (brs, 2 H, c), 7.52-7.45 (m, 4 H, *naphthyl*), 7.37 (d, J = 8.0 Hz, 2 H, h), 6.99 (brs, 2 H, d), 6.38 (d, J = 8.0 Hz, 2 H, i), 2.55 (s, 6 H, e). ^{13}C NMR (100 MHz, CD_3CN, r.t., δ / ppm) : δ 166.1 (C15), 151.8 (C1), 150.2 (C3), 147.4 (C6), 145.2 (C8), 138.1 (C16), 135.8 (C19), 133.9 (C18), 132.5 (C11), 132.4 (C10), 129.1 (*naphthyl*), 128.5 (*naphthyl*), 128.1 (*naphthyl*), 127.6 (*naphthyl*), 126.5 (C9), 126.0 (C7), 125.2 (C17), 124.9 (C2), 123.6 (C4), 121.4 (C13), 20.5 (py-CH_3). C14 and carbonyl carbon peaks were not observed due to broadening of the peaks by introducing Mn. ESI-MS (CH_3CN) : m/z = 1211.2 [(**1-Me**)Mn$(CO)_2(CH_3CN)_2$]$^+$.
Anal. Found (calcd for $C_{55}H_{36}BBr_3F_4IrMnN_6O_3$): C, 47.36 (47.10); H, 3.07 (2.59); N, 6.10 (5.99).

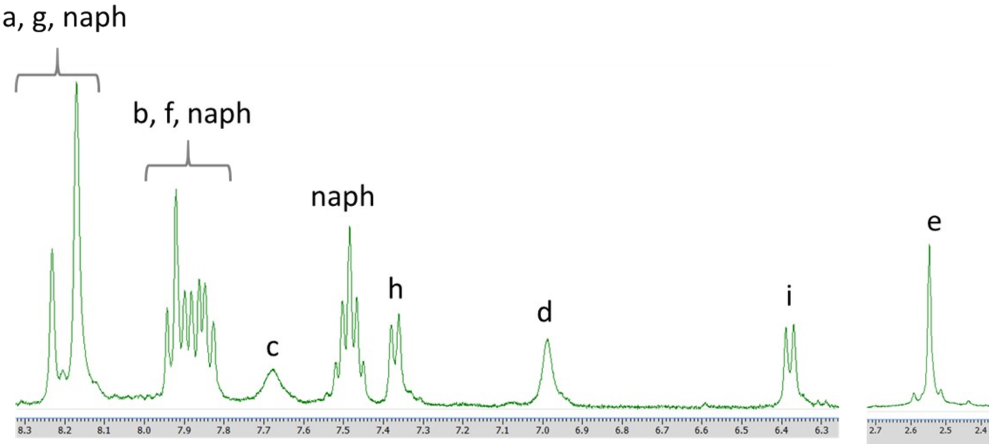

Figure S8. ^{1}H NMR spectra of **3-Me** (400 MHz, r.t., CD_3CN).

Preparation of [Ir(**L1**)$_2$(bpm^{Br})Ir(cod)]$(BF_4)_2$.

[Ir(L1)$_2$(bpm^{Br})](BF_4) (60.0 mg, 0.0507 mmol) was dissolved in acetone (3 mL) and acetone (3 mL) solution of [Ir$(cod)_2$]BF_4 (26.4 mg, 0.0532 mmol, 1.05 eq) was added. The mixture was stirred at ambient temperature for 3 h. The resulting solution was concentrated under vacuum and precipitated with acetone-Et_2O. It gave the target compound [Ir(L1)$_2$(bpm^{Br})Ir(cod)]$(BF_4)_2$ as a brownish solid (62.0 mg, 0.0395 mmol, 77.9%).
^{1}H NMR (400 MHz, $CDCl_3$, r.t., δ / ppm) : 8.61 (s, 2 H, a), 8.40 (s, 2 H, b), 8.12 (d, J = 5.6 Hz, 2 H, c), 8.03 (s, 2 H, g), 7.99 (s, 2 H, f), 7.91 – 7.85 (m, 8 H, *naphthyl*), 7.73 (d, J = 8.8 Hz, 2 H, *naphthyl*), 7.51 – 7.45 (m, 4 H, *naphthyl*), 7.35 (d, J = 8.0 Hz, 2 H, h), 7.27 (d, J = 5.6 Hz, 2 H, d), 6.36 (d, J = 8.0 Hz, 2 H, i), 4.94 (brs, 2 H, cod), 4.47 (brs, 2 H, cod), 2.66 – 2.58 (m, 8 H, e, cod), 2.51 – 2.41 (m, 2 H, cod), 2.12 – 2.04 (m, 2 H, cod), 1.96 – 1.89 (m, 2 H, cod).

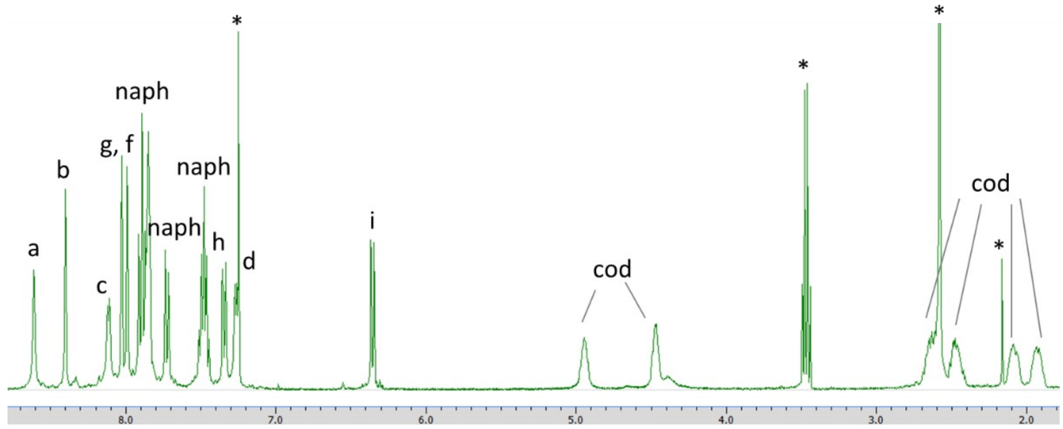

Figure S9. ^{1}H NMR spectra of [Ir(**L1**)$_2$(bpm^{Br})Ir(cod)](BF_4)$_2$ (400 MHz, r.t., $CDCl_3$).

Preparation of [Ir(**L1**)$_2$(bpm^{Br})Ir(PPh_3)$_2$$H_2$]($BF_4$)$_2$ (**4-Me**).

[Ir(**L1**)$_2$(bpm^{Br})Ir(cod)](BF_4)$_2$ (62.0 mg, 0.0395 mmol) was dissolved in CH_2Cl_2 (2.0 mL) and H_2 gas was introduced (1 atm, 2 L balloon) after degassing by freeze-pump-thaw method. After stirring 30 minutes in H_2 atmosphere, CH_2Cl_2 (1 mL) solution of PPh_3 (20.7 mg, 0.0790 mmol, 2 eq) was added and stirred overnight. The resulting solution was concentrated under vacuum and precipitated with CH_2Cl_2 – hexane. The resulting solid was washed with Et_2O to remove free PPh_3. The target compound [Ir(**L1**)$_2$(bpm^{Br})Ir(PPh_3)$_2$(H)$_2$](BF_4)$_2$ as a dark-brown solid (49.9 mg, 0.0251 mmol, 63.6%).

^{1}H NMR (400 MHz, $CDCl_3$, r.t., δ / ppm) : 8.35 (s, 2 H, a), 8.12 (s, 2 H, b), 8.05 (s, 2 H, *naphthyl*), 8.04 (s, 2 H, g), 7.98 (s, 2 H, f), 7.90 – 7.83 (m, 8 H, *naphthyl*), 7.74 (d, J = 8.0 Hz, 2 H, h), 7.67 (d, J = 5.6 Hz, 2 H, c), 7.51 – 7.44 (m, 4 H, *naphthyl*), 7.37 – 7.32 (m, 20 H, d, P*Ph$_3$*), 7.17 – 7.13 (m, 12 H, P*Ph$_3$*), 6.37 (d, J = 8.0 Hz, 2 H, i), 2.65 (s, 6 H, e), -19.9 (t, J = 16 Hz, 2 H, Ir-*H*). ^{13}C NMR (100 MHz, CD_3NO_2, r.t., δ / ppm) : δ 166.5 (C15), 161.7 (C14), 161.1 (C5), 157.6 (C12), 153.4 (C1), 148.8 (C3), 144.7 (C6), 143.1 (C8), 137.8 (C16), 136.7 (C19), 133.9 (C18), 132.9-132.7 (P*Ph$_3$*), 132.1 (C11), 131.5 (C10), 130.5-130.0 (P*Ph$_3$*), 129.3 (*naphthyl*), 129.0-128.9 (P*Ph$_3$*), 128.6 (*naphthyl*), 128.1 (*naphthyl*), 127.6 (*naphthyl*), 127.5 (*naphthyl*), 126.6 (*naphthyl*), 126.1 (C9), 125.5 (C7), 124.9 (C17), 124.8 (C2), 123.6 (C4), 122.1 (C13), 20.3 (py-*C*H$_3$). ^{31}P{^{1}H} NMR (162 MHz, $CDCl_3$, r.t., δ/ppm): δ 19.6 (s). Anal. Found (calcd for $C_{88}H_{68}B_2Br_2F_8Ir_2N_6P_2$ + CH_2Cl_2) : C; 51.17 (51.53), H; 3.57 (3.40), N; 3.88 (4.05).

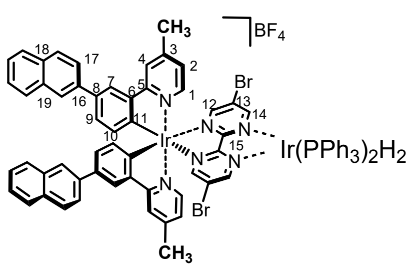

carbon label

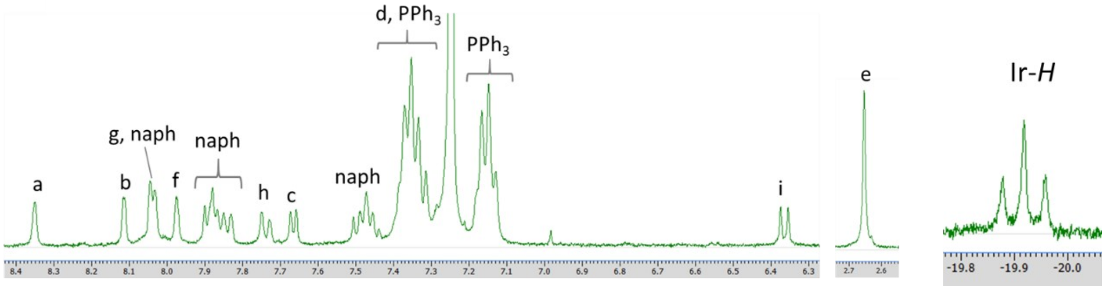

Figure S10. ^{1}H NMR spectra of **4-Me** (400 MHz, r.t., $CDCl_3$).

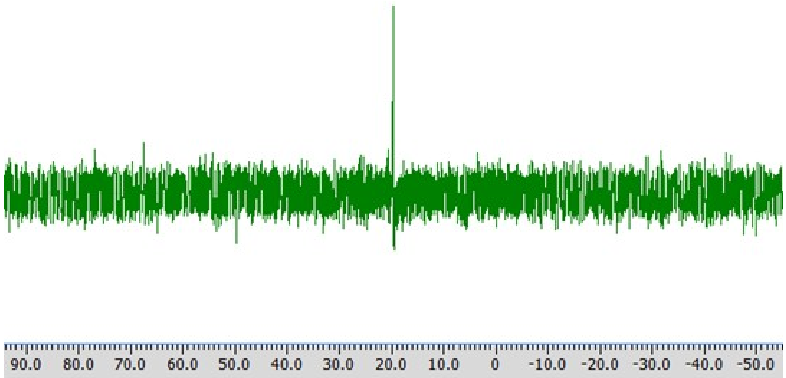

Figure S11. $^{31}P\{^{1}H\}$ NMR spectra of **4-Me** (162 MHz, r.t., $CDCl_3$).

Photochemical Catalytic Reaction.

A CD_3NO_2 solution (0.4 mL) of styrene (0.5 mol/l) with a catalytic amount of the catalyst **1** (1 mol%) was prepared in a 5ϕ NMR glass tube under nitrogen atmosphere. For visible-light irradiation, the tube was placed at a distance of 60 mm from a light source (150 W Xe lamp with a L42 cut-off filter ($\lambda > 420$ nm) and a cold filter ($\lambda < 730$ nm)). For the dark condition, the tube was foiled with an aluminum sheet and placed at the same position as the irradiation experiment. Reactions were followed by ^{1}H NMR spectroscopy after appropriate time intervals.

For copolymerization of styrenes, a CD_3NO_2 solution (0.4 mL) of both the substrates (50 equiv/cat, each) with a catalytic amount of the Ir-Pd complex (1 mol%) was prepared, then irradiated or kept dark, under the same condition.

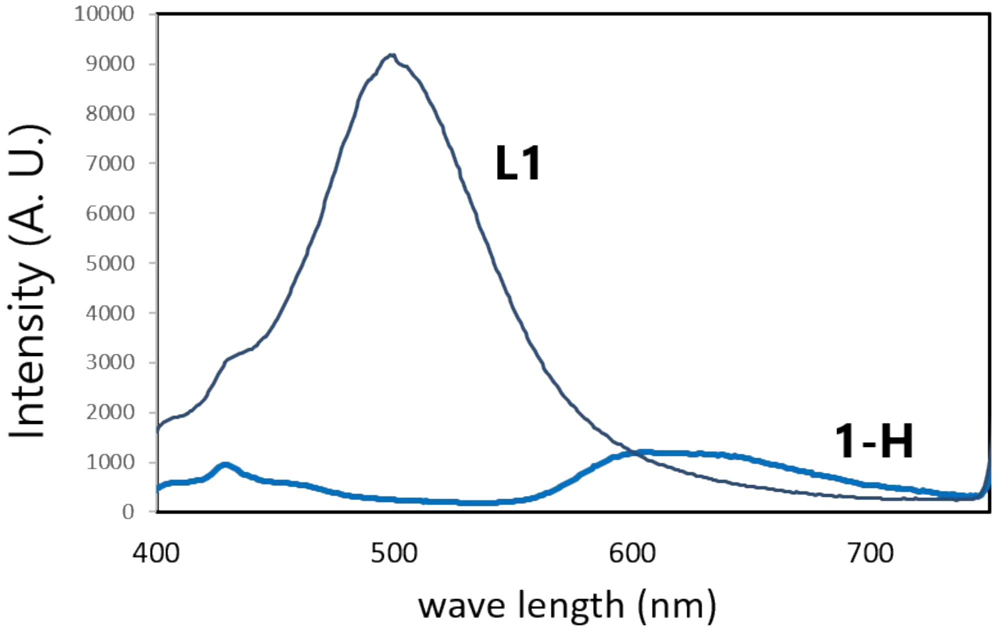

Figure S12. Emission spectra (λ_{ex} = 380 nm, O.D. = 0.1) of **L1** and **1-H** measured in CH_3CN at ambient temperature.

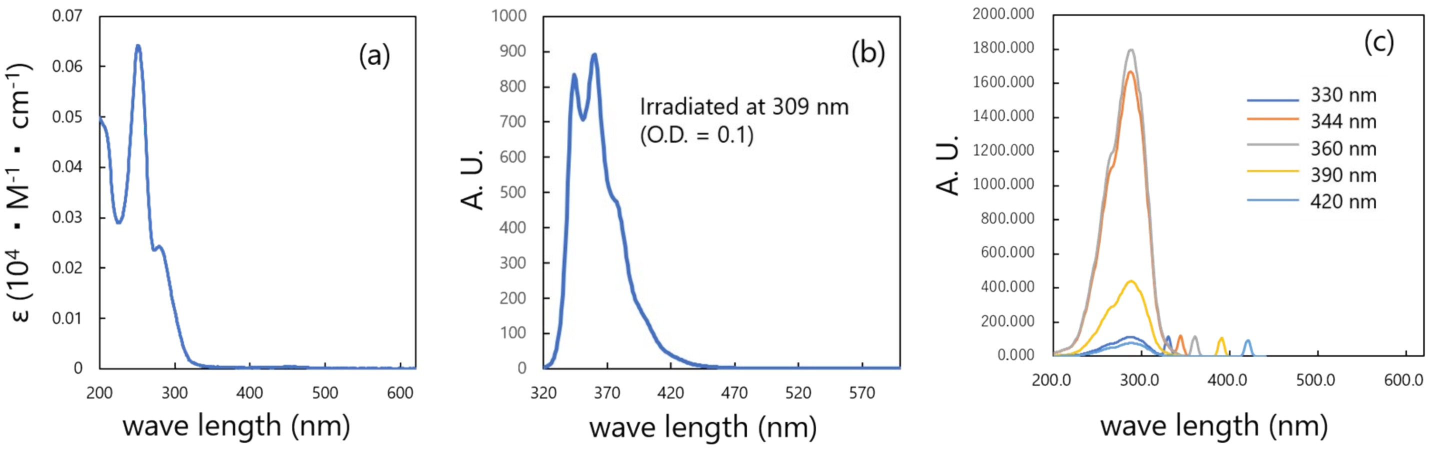

Figure S13. (a) Absorption spectrum, (b) emission spectrum (excitation at 309 nm, O.D. = 0.1), and (c) excitation spectra of **L1** measured in CH_3CN at r.t.

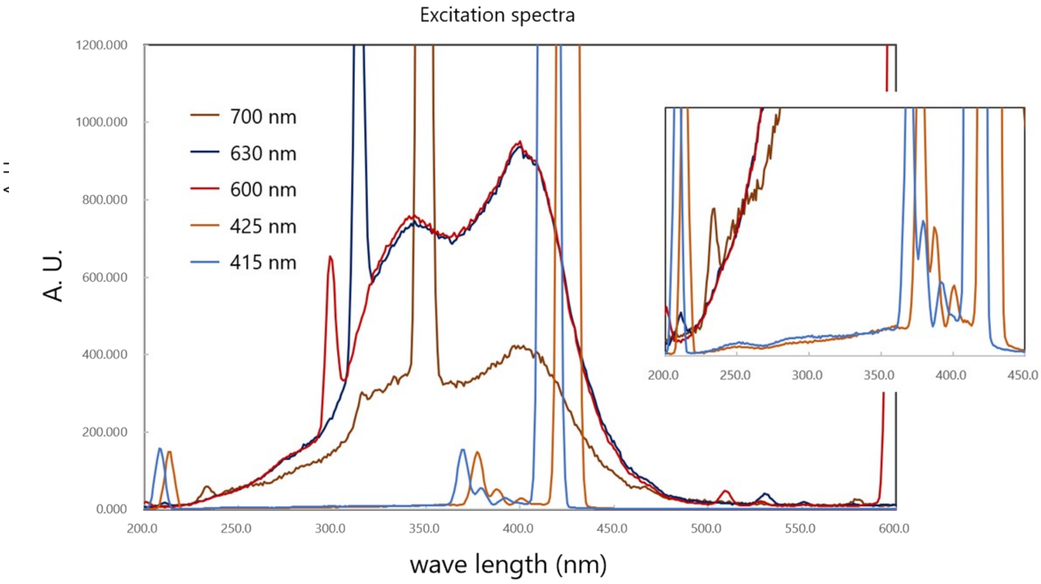

Figure S14. Excitation spectra of **1-Me** measured in CH_3CN at r.t.

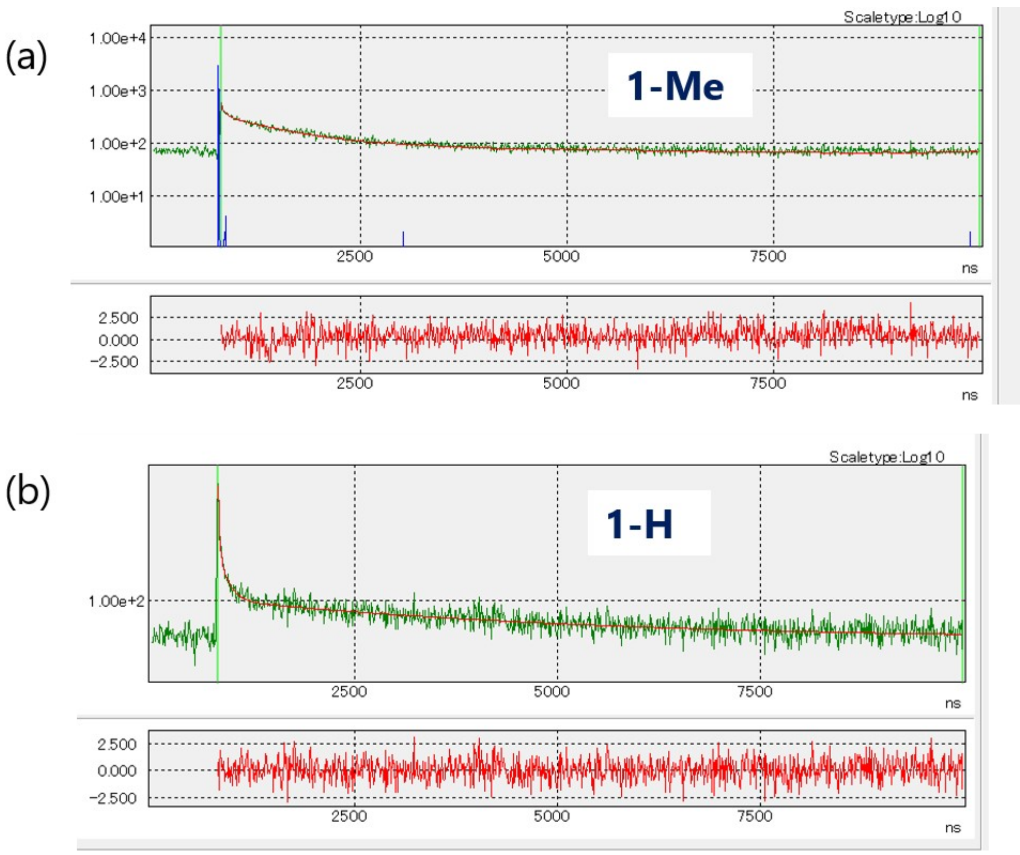

Figure S15. Emission decay curve vs time of (a) **1-Me** and (b) **1-H** measured in CH_3CN at r.t. (λ_{irr} = 365 nm, λ_{det} 640 nm).

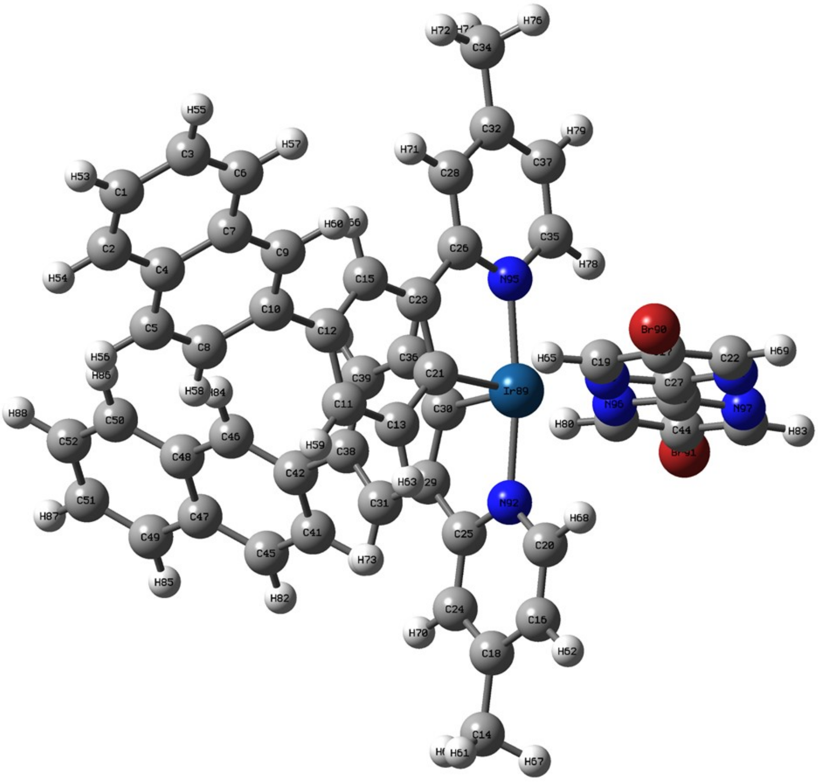

Figure S16. Optimized structure of **1-Me** cation.

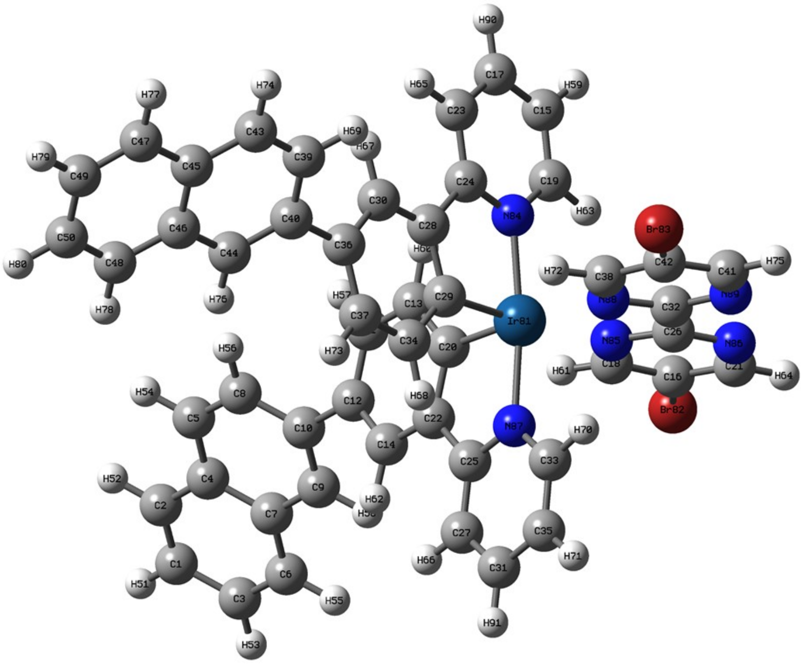

Figure S17. Optimized structure of **1-H** cation.

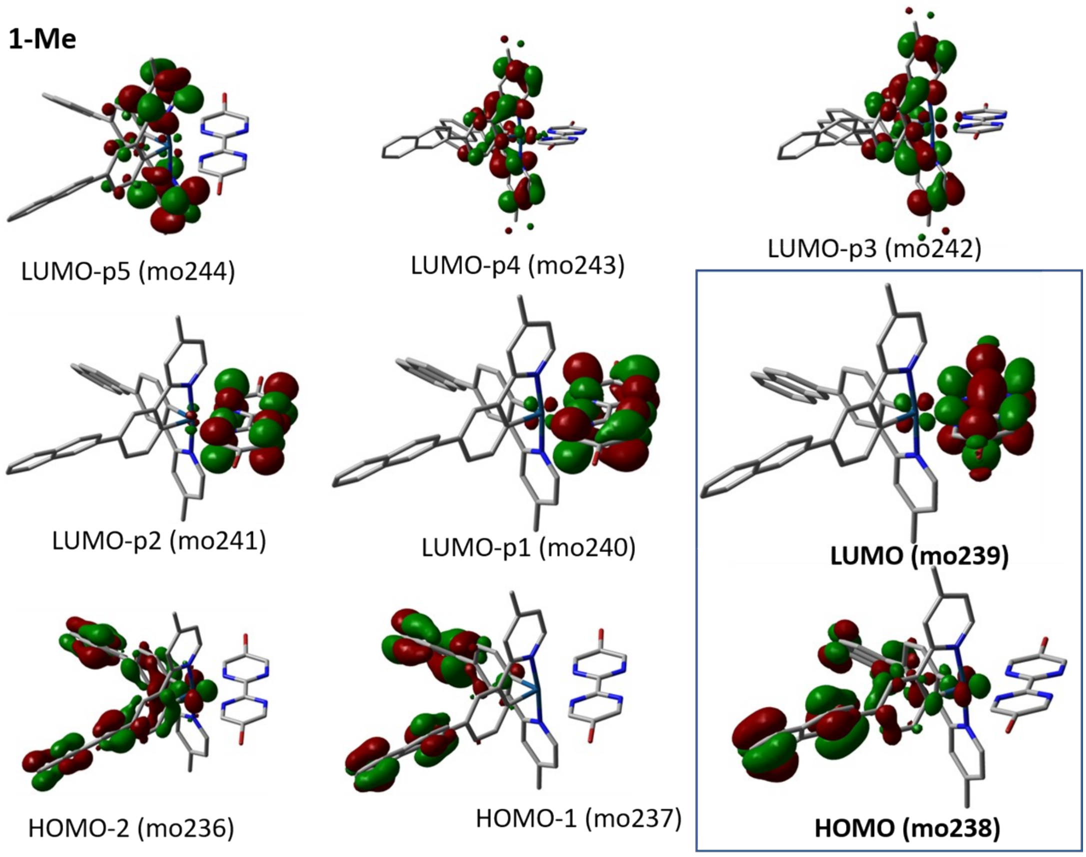

Figure S18. Frontier and energetically nearby orbitals of **1-Me**.

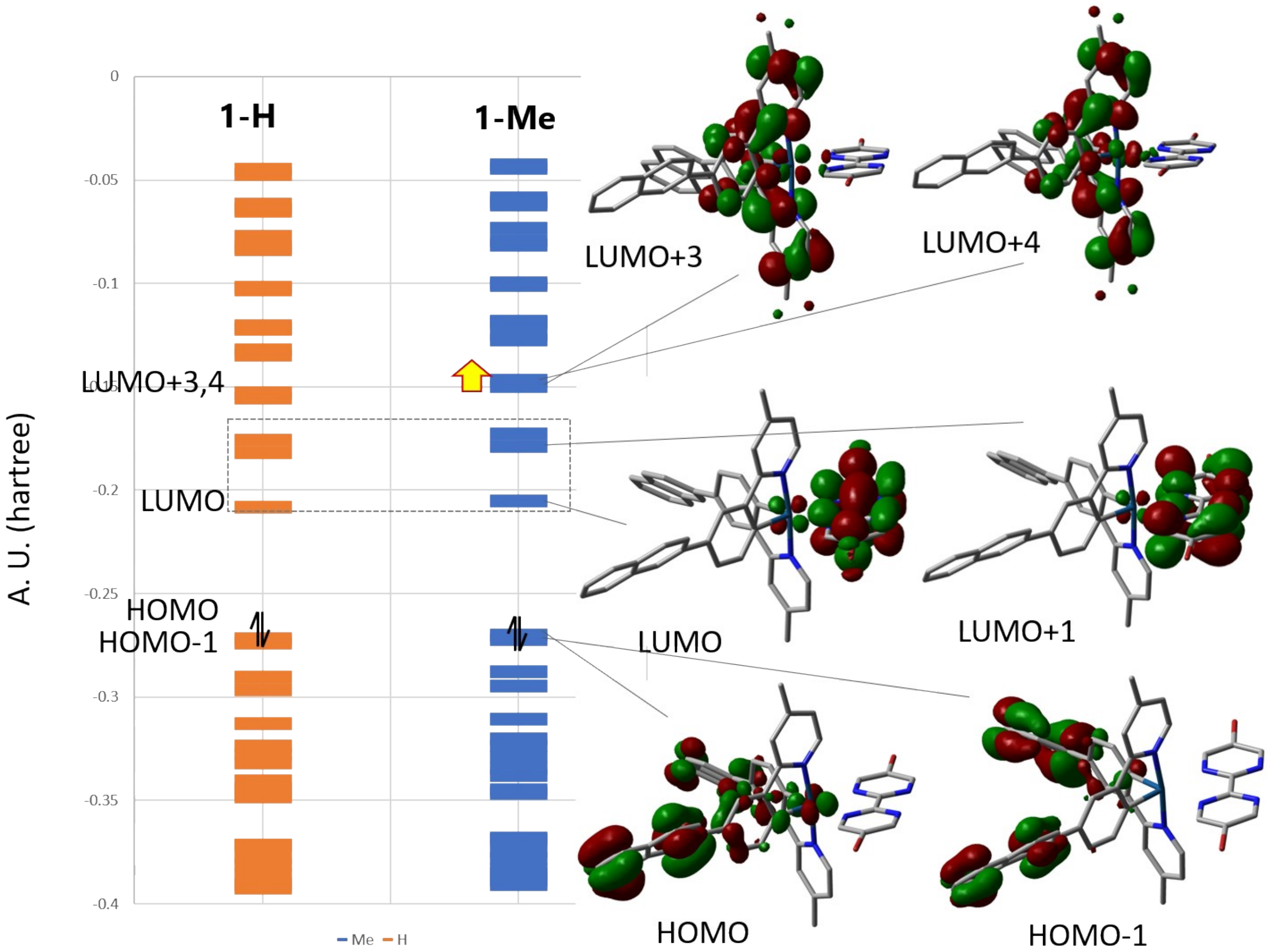

Figure S19. Selected MO energy of **1-Me** and **1-H.**

Table S3. XYZ coordinate of optimized structure of **1-Me**.

6	8.670777000	6.148056000	0.065113000
6	7.482205000	6.336954000	0.733322000
6	8.885391000	4.971386000	-0.697348000
6	6.451723000	5.359710000	0.670518000
6	5.211349000	5.515249000	1.349525000
6	7.907686000	4.006451000	-0.779377000
6	6.665573000	4.171582000	-0.104498000
6	4.234514000	4.552413000	1.270799000
6	5.635895000	3.195444000	-0.165652000
6	4.436265000	3.367568000	0.502130000
6	2.655394000	1.948449000	1.580546000
6	3.364218000	2.339561000	0.428959000
6	1.651007000	0.979740000	1.520271000
6	-2.340738000	-0.917335000	5.973328000
6	3.029247000	1.733787000	-0.785688000
6	-0.695212000	-1.831462000	4.270183000
6	3.456409000	-3.887663000	0.424235000
6	-1.781204000	-0.988612000	4.570182000
6	2.671562000	-2.737757000	0.401215000
6	-0.201359000	-1.869313000	2.977475000
6	1.314023000	0.358376000	0.313949000
6	2.834317000	-5.117851000	0.209956000
6	2.021455000	0.757503000	-0.845586000
6	-2.308550000	-0.225163000	3.531360000
6	-1.773445000	-0.295718000	2.236924000
6	1.611029000	0.094504000	-2.089285000
6	0.812731000	-4.042900000	-0.029029000
6	2.131868000	0.358492000	-3.364398000
6	-2.241703000	0.471846000	1.076521000
6	-1.509807000	0.268042000	-0.118134000
6	-3.326618000	1.362241000	1.124972000
6	1.662910000	-0.319313000	-4.487212000
6	-0.647530000	-4.088448000	-0.283587000
6	2.207686000	-0.040278000	-5.870103000
6	0.168498000	-1.505193000	-3.014506000

6	-1.903986000	0.992810000	-1.246815000
6	0.650822000	-1.277093000	-4.291930000
6	-3.714239000	2.077116000	-0.012543000
6	-2.985151000	1.875888000	-1.199619000
6	-2.609308000	-2.899717000	-0.570118000
6	-6.060691000	2.663813000	0.711388000
6	-4.858404000	3.025909000	0.033983000
6	-2.574827000	-5.291246000	-0.655512000
6	-3.296936000	-4.099907000	-0.729848000
6	-7.126403000	3.529191000	0.768077000
6	-4.775519000	4.268281000	-0.569596000
6	-7.062911000	4.811302000	0.155279000
6	-5.858841000	5.185457000	-0.529152000
6	-8.147022000	5.729948000	0.196395000
6	-5.786090000	6.469603000	-1.138603000
6	-8.045184000	6.963062000	-0.406798000
6	-6.853365000	7.336181000	-1.079511000
1	9.451181000	6.897682000	0.118867000
1	7.315222000	7.234667000	1.318709000
1	9.827583000	4.837603000	-1.215539000
1	5.043530000	6.418305000	1.926544000
1	8.070600000	3.105298000	-1.361147000
1	3.284506000	4.697697000	1.771714000
1	2.909242000	2.400098000	2.533209000
1	5.817345000	2.285776000	-0.729245000
1	-1.572090000	-0.568368000	6.672886000
1	-0.239750000	-2.445969000	5.036153000
1	1.129391000	0.714459000	2.434472000
1	-3.190935000	-0.232800000	6.025735000
1	3.085524000	-1.749345000	0.558986000
1	3.547364000	2.052392000	-1.683034000
1	-2.671172000	-1.908366000	6.305257000
1	0.638971000	-2.500237000	2.718975000
1	3.391699000	-6.045387000	0.217890000
1	-3.138817000	0.441089000	3.722241000
1	2.904004000	1.107986000	-3.472835000

1	2.995869000	0.716029000	-5.839443000
1	-3.865137000	1.528309000	2.051114000
1	1.408812000	0.319105000	-6.529306000
1	-1.369148000	0.875705000	-2.184101000
1	2.620417000	-0.954927000	-6.311317000
1	-6.135402000	1.679080000	1.158611000
1	-0.616183000	-2.228445000	-2.834786000
1	0.242917000	-1.833373000	-5.126160000
1	-3.104011000	-1.937193000	-0.615207000
1	-3.284774000	2.408336000	-2.095464000
1	-8.040828000	3.239273000	1.274637000
1	-3.054009000	-6.254352000	-0.773288000
1	-3.858182000	4.570362000	-1.064179000
1	-9.056375000	5.441962000	0.712811000
1	-4.873456000	6.753177000	-1.651845000
1	-8.875856000	7.657719000	-0.370214000
1	-6.789468000	8.311361000	-1.547476000
77	-0.039772000	-1.107981000	0.015387000
35	5.356588000	-3.769230000	0.744937000
35	-5.201743000	-4.101942000	-1.045064000
7	-0.719686000	-1.126292000	1.976324000
7	1.347688000	-2.815779000	0.179586000
7	1.509155000	-5.184947000	-0.016820000
7	0.629827000	-0.843831000	-1.931516000
7	-1.282567000	-2.893601000	-0.351787000
7	-1.247668000	-5.274820000	-0.431151000

Table S4. XYZ coordinate of optimized structure of **1-H**.

6	8.623040000	6.193331000	-0.247170000
6	7.453869000	6.379761000	0.455080000
6	8.823647000	5.011104000	-1.004847000
6	6.429628000	5.394258000	0.432649000
6	5.209138000	5.547160000	1.147345000
6	7.851535000	4.038065000	-1.048154000
6	6.629254000	4.200417000	-0.337394000
6	4.237689000	4.576537000	1.107153000

6	5.605686000	3.216251000	-0.358431000
6	4.425461000	3.386132000	0.343619000
6	2.686672000	1.965256000	1.486996000
6	3.359381000	2.349914000	0.311609000
6	1.687192000	0.989768000	1.465494000
6	2.993647000	1.730104000	-0.886813000
6	-0.555501000	-1.822103000	4.303886000
6	3.487084000	-3.882905000	0.364419000
6	-1.633590000	-0.983689000	4.610157000
6	2.696160000	-2.736826000	0.353637000
6	-0.099864000	-1.863216000	2.994062000
6	1.319711000	0.354581000	0.275611000
6	2.864926000	-5.117519000	0.176735000
6	1.990984000	0.746497000	-0.907520000
6	-2.207302000	-0.224126000	3.599869000
6	-1.708508000	-0.300114000	2.289519000
6	1.549900000	0.069729000	-2.131535000
6	0.832327000	-4.053736000	-0.015034000
6	2.033232000	0.322110000	-3.425470000
6	-2.213029000	0.455121000	1.137986000
6	-1.514538000	0.245902000	-0.075450000
6	-3.301097000	1.340442000	1.211375000
6	1.524109000	-0.379302000	-4.509725000
6	-0.634391000	-4.108737000	-0.228237000
6	0.083185000	-1.551103000	-2.996981000
6	-1.944675000	0.959821000	-1.197665000
6	0.526521000	-1.337107000	-4.294144000
6	-3.725176000	2.044159000	0.080095000
6	-3.029128000	1.837299000	-1.125895000
6	-2.610080000	-2.933274000	-0.471043000
6	-6.052160000	2.624391000	0.868460000
6	-4.872795000	2.987069000	0.152246000
6	-2.564579000	-5.325175000	-0.535781000
6	-3.295413000	-4.138512000	-0.601030000
6	-7.120186000	3.484888000	0.949939000
6	-4.814481000	4.224583000	-0.464041000

6	-7.081794000	4.762114000	0.324984000
6	-5.900900000	5.136610000	-0.398561000
6	-8.168957000	5.675627000	0.391384000
6	-5.853222000	6.415907000	-1.020512000
6	-8.091734000	6.904135000	-0.224711000
6	-6.922779000	7.277561000	-0.936245000
1	9.398827000	6.949281000	-0.224214000
1	7.297722000	7.281765000	1.036813000
1	9.750637000	4.879585000	-1.550276000
1	5.051881000	6.454420000	1.720696000
1	8.003718000	3.132783000	-1.626378000
1	3.302122000	4.719868000	1.635088000
1	2.964798000	2.428003000	2.427431000
1	5.777159000	2.302721000	-0.918914000
1	-0.075753000	-2.427130000	5.060852000
1	1.194119000	0.731095000	2.397240000
1	3.109781000	-1.745434000	0.492564000
1	3.483358000	2.043557000	-1.801760000
1	0.736469000	-2.488473000	2.711039000
1	3.426512000	-6.042553000	0.176571000
1	-3.035295000	0.436674000	3.813781000
1	2.798014000	1.072323000	-3.567982000
1	-3.813726000	1.511179000	2.151262000
1	-1.436620000	0.839163000	-2.149265000
1	-6.108470000	1.643135000	1.325902000
1	-0.692743000	-2.273765000	-2.781909000
1	0.098580000	-1.902661000	-5.110373000
1	-3.111394000	-1.973962000	-0.511433000
1	-3.357211000	2.361153000	-2.016777000
1	-8.017384000	3.194699000	1.486220000
1	-3.041216000	-6.291994000	-0.631417000
1	-3.914060000	4.527283000	-0.988459000
1	-9.060744000	5.387501000	0.937460000
1	-4.958042000	6.699761000	-1.563456000
1	-8.924497000	7.594960000	-0.168676000
1	-6.878205000	8.249083000	-1.413918000

77	-0.033940000	-1.121557000	0.028232000
35	5.394163000	-3.753120000	0.632467000
35	-5.207597000	-4.153384000	-0.863686000
7	-0.655967000	-1.128004000	2.008080000
7	1.367130000	-2.822572000	0.168601000
7	1.534313000	-5.192300000	-0.012828000
7	0.576822000	-0.872924000	-1.939475000
7	-1.277898000	-2.918049000	-0.289233000
7	-1.231797000	-5.299432000	-0.348510000
1	-2.013214000	-0.924362000	5.622522000
1	1.891621000	-0.184160000	-5.509412000

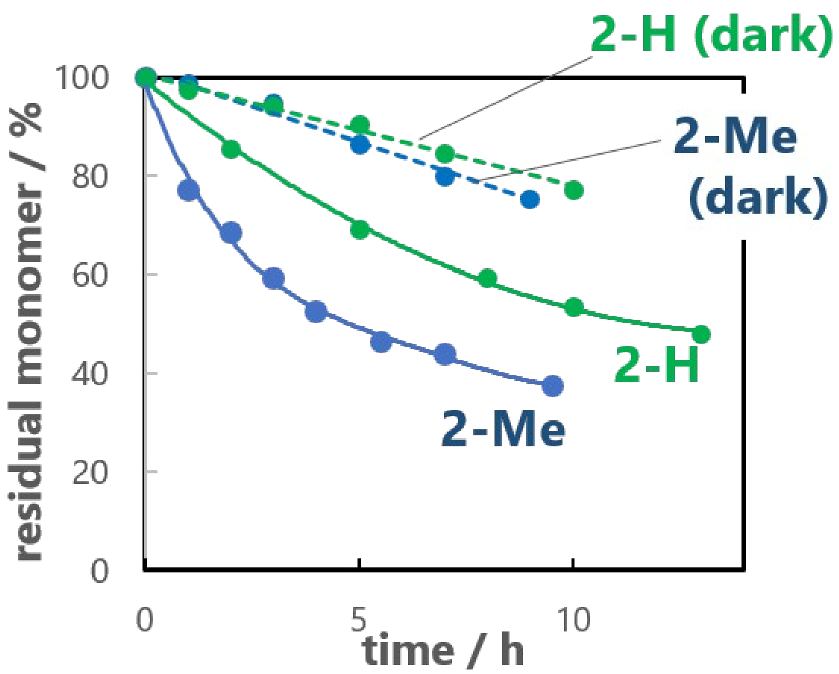

Figure S20. Residual monomer % in photocatalytic styrene polymerization by **2-Me** and **1-Me**. Catlyst 1 mol%, CH_3NO_2 solution under irradiated (solid line) or dark (dotted line) condition. Polymers obtained under irradiated conditions. M_n = *ca.* 5000、M_w / M_n = 1.4-1.5.

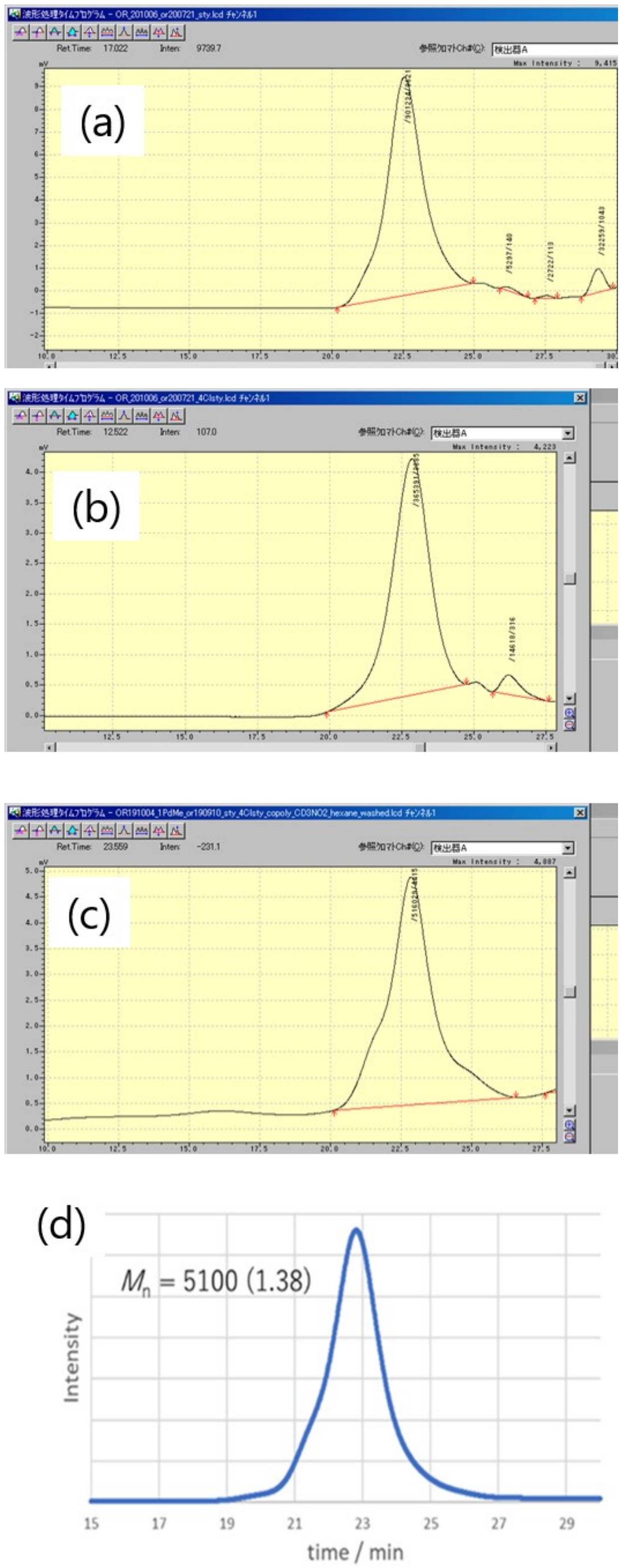

Figure S21**.** GPC traces of crude polymers catalyzed by **2-Me**. (a) polystyrene, (b) 4-chlorostyrene, (c) styrene-4-Cl-styrene copolymer, and (d) 4-Cl-styrene/styrene copolymer after hexane and CH_2Cl_2 wash.

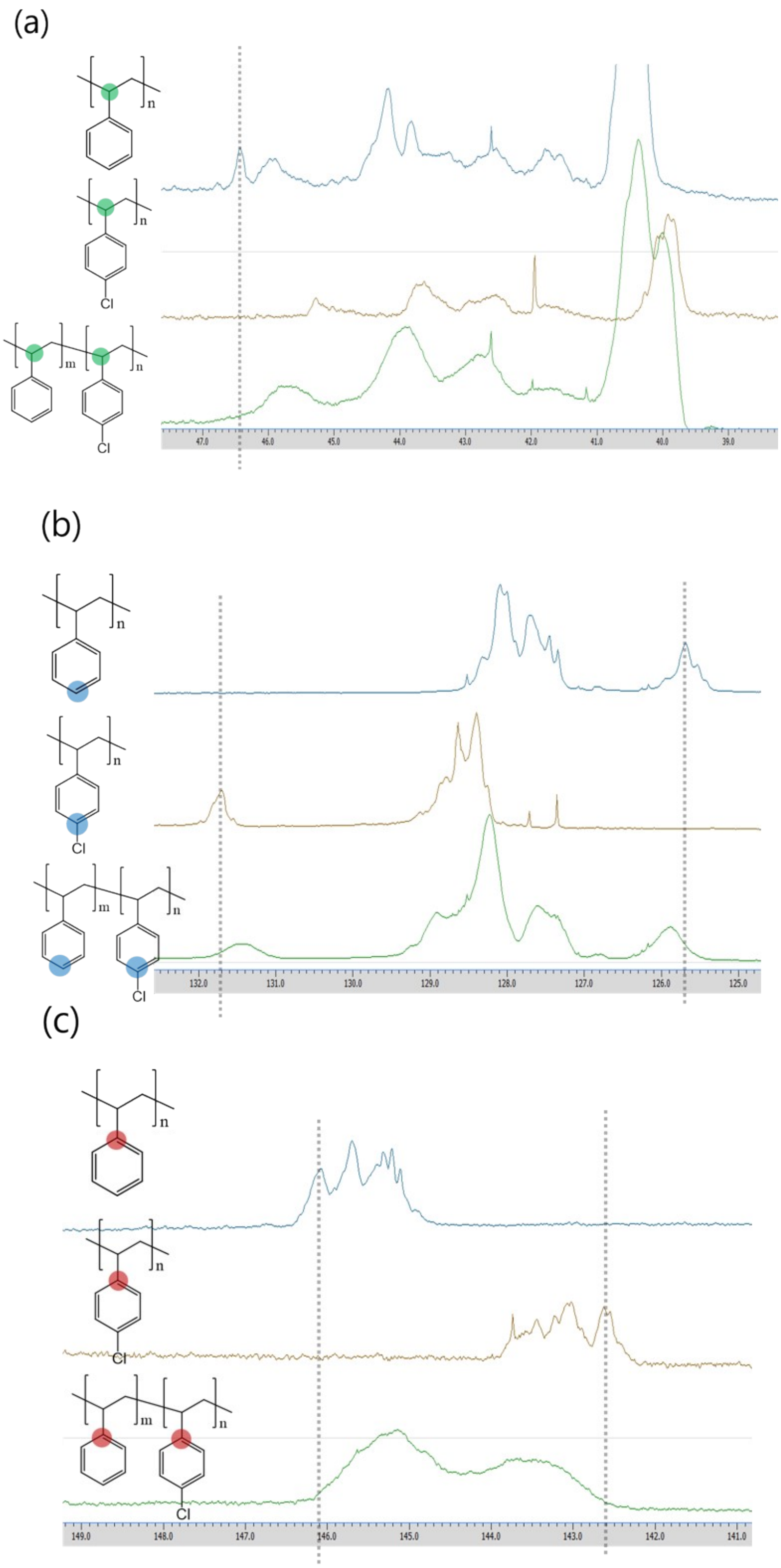

Figure S22. Selected ^{13}C NMR spectral data of polystyrene (blue), poly-*p*-Cl-styrene (brown), and polystyrene-*co*-poly-*p*-Cl-styrene (green). (a) Methine carbon region, (b) aromatic carbon region (*p*-), and (c) aromatic *ipso*-carbon region.

Electronic Supporting Information

References

1. Peng, X.; Wu, Q.; Jiang, S.; Hanif, M.; Chen, S.; Hou, H., High dielectric constant polyimide derived from 5,5′-bis[(4-amino) phenoxy]-2,2′-bipyrimidine. *Journal of Applied Polymer Science* **2014,** *131* (24).

2. Rulke, R. E.; Ernsting, J. M.; Spek, A. L.; Elsevier, C. J.; van Leeuwen, P. W. N. M.; Vrieze, K., NMR study on the coordination behavior of dissymmetric terdentate trinitrogen ligands on methylpalladium(II) compounds. *Inorganic Chemistry* **1993,** *32* (25), 5769-5778.

3. Liu, S.-J.; Zhao, Q.; Fan, Q.-L.; Huang, W., A Series of Red-Light-Emitting Ionic Iridium Complexes: Structures, Excited State Properties, and Application in Electroluminescent Devices. *European Journal of Inorganic Chemistry* **2008,** *2008* (13), 2177-2185.

4. Inagaki, A.; Edure, S.; Yatsuda, S.; Akita, M., Highly selective photo-catalytic dimerization of α-methylstyrene by a novel palladium complex with photosensitizing ruthenium(ii) polypyridyl moiety. *Chemical Communications* **2005,** (43), 5468-5470.

(i) Frisch, M. J.; Trucks, G. W.; Schlegel, H. B.; Scuseria, G. E.; Robb, M. A.; Cheeseman, J. R.; Scalmani, G.; Barone, V.; Petersson, G. A.; Nakatsuji, H.; Li, X.; Caricato, M.; Marenich, A. V.; Bloino, J.; Janesko, B. G.; Gomperts, R.; Mennucci, B.; Hratchian, H. P.; Ortiz, J. V.; Izmaylov, A. F.; Sonnenberg, J. L.; Williams-Young, D.; Ding, F.; Lipparini, F.; Egidi, F.; Goings, J.; Peng, B.; Petrone, A.; Henderson, T.; Ranasinghe, D.; Zakrzewski, V. G.; Gao, J.; Rega, N.; Zheng, G.; Liang, W.; Hada, M.; Ehara, M.; Toyota, K.; Fukuda, R.; Hasegawa, J.; Ishida, M.; Nakajima, T.; Honda, Y.; Kitao, O.; Nakai, H.; Vreven, T.; Throssell, K.; Montgomery, J. A., Jr.; Peralta, J. E.; Ogliaro, F.; Bearpark, M. J.; Heyd, J. J.; Brothers, E. N.; Kudin, K. N.; Staroverov, V. N.; Keith, T. A.; Kobayashi, R.; Normand, J.; Raghavachari, K.; Rendell, A. P.; Burant, J. C.; Iyengar, S. S.; Tomasi, J.; Cossi, M.; Millam, J. M.; Klene, M.; Adamo, C.; Cammi, R.; Ochterski, J. W.; Martin, R. L.; Morokuma, K.; Farkas, O.; Foresman, J. B.; Fox D. J. Gaussian 16, Revision A.03, Gaussian, Inc., Wallingford, CT, 2016.

(ii) (a) Becke, A. D. Density-Functional Exchange-Energy Approximation with Correct Asymptotic Behavior. *Phys. Rev. A* **1988**, *38*, 3098–3100; (b) Becke, A. D. Density-Functional Thermochemistry. III. The Role of Exact Exchange. *J. Chem. Phys.* **1993**, *98*, 5648–5652; (c) Lee, C.; Yang, W.; Parr, R. G. Development of the Colle-Salvetti Correlation-Energy Formula into a Functional of the Electron Density. *Phys. Rev. B* **1988**, *37*, 785–789.

(iii) (a) Dunning, T. H., Jr.; Hay, P. J. In *Modern Theoretical Chemistry*; Schaefer, H. F., III, Ed.; Plenum: New York, 1976; Vol. 3, pp 1–28; (b) Hay, P. J.; Wadt, W. R. *Ab Initio* Effective Core Potentials for Molecular Calculations. Potentials for the Transition Metal Atoms Sc to Hg. *J. Chem. Phys.* **1985**, *82*, 270–283; (c) Hay, P. J.; Wadt, W. R. *Ab Initio* Effective Core Potentials for Molecular Calculations. Potentials for K to Au Including the Outermost Core Orbitals. *J. Chem. Phys.* **1985**, *82*, 299–310; (d) Wadt, W. R.; Hay, P. J. *Ab Initio* Effective Core Potentials for Molecular Calculations. Potentials for Main Group Elements Na to Bi. *J. Chem. Phys*. **1985**, *82*, 284–298.

(iv) Petersson, G. A.; Bennett, A.; Tensfeldt, T. G.; Al-Laham, M. A.; Shirley, W. A.; Mantzaris, J. A Complete Basis Set Model Chemistry. I. The Total Energies of Closed-Shell Atoms and Hydrides of the First-Row Elements. *J. Chem. Phys.* **1988**, *89*, 2193–2218.

(v) Binkley, J. S.; Pople, J. A.; Hehre, W. J. Self-Consistent Molecular Orbital Methods. 21. Small Split-Valence Basis Sets for First-Row Elements. *J. Am. Chem. Soc.* **1980**, *102*, 939–947.